COORDINATED PATH-FOLLOWING IN THE PRESENCE OF COMMUNICATION LOSSES AND TIME DELAYS[*]

R. GHABCHELOO[†], A. P. AGUIAR[†], A. PASCOAL[†], C. SILVESTRE[†], I. KAMINER[‡], AND J. HESPANHA[§]

Abstract. This paper addresses the problem of steering a group of vehicles along given spatial paths while holding a desired time-varying geometrical formation pattern. The solution to this problem, henceforth referred to as the coordinated path-following (CPF) problem, unfolds in two basic steps. First, a path-following (PF) control law is designed to drive each vehicle to its assigned path, with a nominal speed profile that may be path dependent. This is done by making each vehicle approach a virtual target that moves along the path according to a conveniently defined dynamic law. In the second step, the speeds of the virtual targets (also called coordination states) are adjusted about their nominal values so as to synchronize their positions and achieve, indirectly, vehicle coordination. In the problem formulation, it is explicitly considered that each vehicle transmits its coordination state to a subset of the other vehicles only, as determined by the communications topology adopted. It is shown that the system that is obtained by putting together the PF and coordination subsystems can be naturally viewed as either the feedback or the cascade connection of the latter two. Using this fact and recent results from nonlinear systems and graph theory, conditions are derived under which the PF and the coordination errors are driven to a neighborhood of zero in the presence of communication losses and time delays. Two different situations are considered. The first captures the case where the communication graph is alternately connected and disconnected (brief connectivity losses). The second reflects an operational scenario where the union of the communication graphs over uniform intervals of time remains connected (uniformly connected in mean). To better root the paper in a nontrivial design example, a CPF algorithm is derived for multiple underactuated autonomous underwater vehicles (AUVs). Simulation results are presented and discussed.

Key words. coordination control, communication losses and time delays, path-following, autonomous underwater vehicles

AMS subject classifications. 93A14, 93D15, 93C85, 93C10, 93A13

DOI. 10.1137/060678993

1. Introduction. Increasingly challenging mission scenarios and the advent of powerful embedded systems, sensors, and communication networks have spawned widespread interest in the problem of coordinated motion control of multiple autonomous vehicles. The types of applications considered are numerous and include aircraft and spacecraft formation control [6], [23], [29], [36], [39], [49], [50], [60], [30], [4], [64], coordinated control of land robots [16], [52], [22], [58], control of multiple surface and underwater vehicles [17], [26], [34], [63], [13], and networked control of robotic systems

[15], [14], [33], [41], [37], [43], [48]. To meet the requirements imposed by these and related applications, a new control paradigm is needed that must necessarily depart from classical centralized control strategies. Centralized controllers deal with systems in which a single controller possesses all the information required to achieve desired control objectives, including stability and performance requirements. In many of the applications envisioned, however, the highly distributed nature of the vehicles' sensing and actuation modules and the constraints imposed by the intervehicle communication network make it impossible to tackle the problems in the framework of centralized control theory. In part due to these reasons, there has been over the past few years a flurry of activity in the area of multiagent networks with application to engineering and science problems. The list of related research topics is vast and includes parallel and distributed computing [7], distributed decision making [61], synchronization in oscillator networks [46], flocking of mobile autonomous agents [5], [18], [28], [54], state agreement and consensus problems [20], [38], [51], [40], [44], [42], [11], asynchronous consensus protocols [9], [61], graph theory and graph connectivity [45], [56], [32], rigidity and persistence in autonomous formations [62], adaptive and distributed coordination algorithms for mobile sensing networks [12], [11], and concurrent synchronization in dynamic system networks [48]. See also [55] and the references therein for general expositions on large-scale dynamical systems and decentralized control of complex systems that bear affinity with the issues addressed in this paper.

In spite of significant progress made in these areas, much work remains to be done to develop strategies capable of yielding robust performance of a fleet of vehicles in the presence of complex vehicle dynamics, severe communication constraints, and partial vehicle failures. These difficulties are especially challenging in the field of marine robotics for two main reasons: (i) often, the dynamics of marine vehicles cannot be greatly simplified for control design purposes; and (ii) underwater communications and positioning rely heavily on acoustic systems, which are plagued with intermittent failures, latency, and multipath effects.

Inspired by recent theoretical and practical developments in the areas of multiple vehicle control, we consider the problem of *coordinated path-following (CPF) control*, where *multiple vehicles are required to follow prespecified paths while keeping a desired, possibly time-varying, geometric formation pattern.* These objectives must be met in the presence of communication losses and delays. The problem arises, for example, in the operation of multiple autonomous underwater vehicles (AUVs) for fast acoustic coverage of the seabed [47]. In this application, two or more vehicles maneuver above the seabed, at either the same or different depths, along geometrically similar spatial paths and map the seabed using identical suites of acoustic sensors. By requesting that the vehicles move along the paths so that the projections of the acoustic beams on the seabed have a certain degree of overlapping, large areas can be mapped in a short time. These objectives impose strict constraints on the vehicle formation pattern.

A number of other scenarios can be envisioned that require CPF control of marine vehicles. Examples include underwater vehicle formation control for 3D vision-based marine habitat mapping, ship underway replenishment [34], and missions where temporal and spatial path deconfliction are critical [30]. Similar problems arise in the area of air vehicle control. All of these scenarios share the requirements that a number of vehicles maneuver along predetermined paths, at nominal speed profiles that may be path dependent, and keep a possibly time-varying formation pattern. Absolute time requirements are not part of the problem. As such, they depart considerably from other related problems such as vehicle rendezvous maneuvers and swarm formation control. The manner in which the paths and the formation are planned depend on

the specific problem at hand, for example, using a time optimality criterion when fast coordinated maneuvering between initial and final positions is required, minimizing an energy-related criterion when the objective is to scan a certain area or volume densely and energy is at a premium, or using a combination of criteria that include geometric constraints when collision avoidance is important. See, for example, [30] for the case of unmanned air vehicles.

In this paper we formulate and solve the problem of CPF by explicitly taking into account the vehicle dynamics and the topology of the underlying communication network, subject to communication losses and delays. The reader is referred to [17], [21], [22], [35], [58] and the references therein for a historical overview of the topic and a perspective of the sequence of motion control problem formulations and solutions upon which the present work builds. See also [19], [57], [47] for an in-depth introductory exposition to the topic at hand. For the sake of clarity, it is important to point out that in the scope of the problem at hand, PF and CPF have also been referred to as output maneuvering and synchronization of multiple maneuvering systems, respectively [58]. A comprehensive survey of related results on consensus in multivehicle cooperative control can be found in [42], [44], and [51].

The solution to the problem of CPF that we propose unfolds in two basic steps. First, a PF control law is designed to drive each vehicle to its assigned path, with a nominal speed profile that may be path dependent. This is done by making each vehicle approach a virtual target that moves along the path according to a conveniently defined dynamic law. Each vehicle has access to a set of local measurements only. In the second step, the speeds of the virtual targets (also called coordination states) are adjusted about their nominal values so as to synchronize their positions and achieve, indirectly, vehicle coordination. The vehicles are allowed to exchange only limited information with their immediate neighbors. Without being too rigorous, it can be said that the strategy proposed abides by a separation principle whereby the PF and coordinated motion control designs are almost decoupled. This simplifies the overall design process. Furthermore, it has the virtue of leaving essentially to each vehicle the task of dealing with external disturbances acting upon it, directly at the PF level.

The mathematical setup adopted in the paper is well rooted in Lyapunov stability and graph theory. At the pure PF level, two types of control laws, henceforth referred to as Type I and Type II, are developed. The difference between them lies in the types of dynamics chosen for the virtual targets along the paths.

Key concepts from input-to-state stability theory [59] are also used to derive results on the *stability, performance, and robustness* of the overall system that results from putting together the PF and vehicle coordination subsystems. Here, we use the fact that combination of the above systems takes either a feedback interconnection or a cascade form, depending on whether the underlying PF laws are of Type I or Type II. The results are quite general in that they apply to a large class of PF control systems satisfying a certain input-to-state stable (ISS) property. For the sake of clarity and completeness, the paper derives a PF strategy for a class of underactuated AUVs that meets the required ISS property.

The key contribution of the paper is the study of the combined behavior of the PF and coordination systems in the presence of temporary communication losses and transmission delays. To deal with communication losses, the paper proposes two frameworks for studying the effect of communication failures and delays on the performance of the overall vehicle formation. The first framework, brief connectivity losses (BCLs), refers to the situation where the communication graph changes in time, alternating between connected and disconnected graphs. Here, we borrow from and

expand previous results on systems with brief instabilities, namely, by deriving a new small-gain theorem that applies to the feedback interconnection of these systems. See [25] and the references therein for an introduction to systems with brief instabilities and their application to control systems analysis and design. The second framework, uniformly connected in mean (UCM), applies to the case where the communication graph may even fail to be connected at any instant of time; however, we assume there is a finite time $T > 0$ such that over any interval of length T the union of the different graphs is connected. This framework is motivated by the work in [37], [38], [40]. To the best of our knowledge, this is the first time that the impact of intermittent failures on coordinated PF is analyzed from a quantitative point of view and estimates on the rate of decay of all closed-loop error signals are obtained. The impact of communication delays on the overall system performance is also analyzed for the case of homogeneous delays and PF systems of Type II. Conditions are derived under which the PF errors become arbitrarily small and the cooperation errors approach zero exponentially. For related results on the consensus problems for systems with nonhomogeneous delays, see [20].

The paper is organized as follows. Section 2 formulates the PF and vehicle coordination problems and describes general stability-related properties that are met by the PF closed-loop subsystem of each vehicle. Section 3 introduces some basic notation, summarizes important results on graph theory, and develops the tools that will be used to study the different types of communication topologies considered in the paper. Section 4 derives a useful small-gain theorem for the feedback interconnection of systems with brief instabilities. Section 5 studies the CPF problem in the case where the communications network is subjected to communication losses with no time delays. Section 6 extends some of the results of section 5 to deal with switching communication networks and time delays. An illustrative example is presented in section 7, where a CPF control algorithm for a general class of underactuated AUVs is derived. The results of simulations are also described. Finally, section 8 contains the main conclusions and describes problems that warrant further research. The proofs of several statements are included in the appendix.

2. Problem statement. This section provides a rigorous formulation of the PF and coordination problems that are the main subjects of the paper. Consider a group of n vehicles numbered $1, \ldots, n$. We let the dynamics of vehicle i be modeled by a general system of the form

(2.1)
$$\dot{x}_i = f_i(x_i, u_i, w_i),$$
$$y_i = h_i(x_i, v_i),$$

where $x_i \in \mathbb{R}^n$ is the state, $u_i \in \mathbb{R}^m$ is the control signal, and $y_i \in \mathbb{R}^q$ is the output that we require to reach and follow a path $y_{d_i}(\gamma_i) : \mathbb{R} \to \mathbb{R}^q$ parameterized by $\gamma_i \in \mathbb{R}$. Signals w_i and v_i denote the disturbance inputs and measurement noises, respectively. Later in section 7, an example will be given where the dynamics of (2.1) are those of a very general class of AUVs. In that case, the output y_i corresponds to the position of the vehicle with respect to an inertial coordinate frame.

For any continuous, differentiable timing law $\gamma_i(t)$, define the PF and speed tracking error variables

(2.2)
$$e_i(t) := y_i(t) - y_{d_i}(\gamma_i(t))$$

and

(2.3)
$$\eta_i(t) := \dot{\gamma}_i(t) - v_{r_i}(t),$$

respectively, where $v_{r_i}(t) \in \mathbb{R}$ denotes a desired temporal speed profile to be defined.

Inspired by the work in [3, 22, 57], we start by defining the problem of PF for each vehicle. In what follows, $\|.\|$ denotes both the Euclidean norm of a vector and the spectral norm of a matrix.

DEFINITION 2.1 (PF problem). *Consider a vehicle with dynamics* (2.1), *together with a spatial path* $y_{d_i}(\gamma_i)$; $\gamma_i \in \mathbb{R}$, *to be followed and a desired, predetermined temporal speed profile* $v_{r_i}(t)$ *to be tracked. Let the PF error and the speed tracking error be as in* (2.2) *and* (2.3), *respectively. Given* $\epsilon > 0$, *design a feedback control law for* u_i *such that all closed-loop signals are bounded and both* $\|e_i\|$ *and* $|\eta_i|$ *converge to a neighborhood of the origin of radius* ϵ.

Stated in simple terms, the problem above amounts to requiring that the output y_i of a vehicle converge to and remain inside a tube centered around the desired path y_{d_i}, while ensuring that its rate of progression $\dot{\gamma}_i$ also converge to and remain inside a tube centered around the desired speed profile $v_{r_i}(t)$.

We assume that the PF controllers adopted meet a number of technical conditions described next. In section 7, as an example, we introduce a PF controller for a general underactuated vehicle that meets these conditions. The interested reader will find in [22], [57], and the references therein related material on PF control of nonlinear systems. See also [3] for an interesting discussion on the possible advantages of PF versus trajectory tracking control. Namely, the fact that PF control for nonminimum phase systems removes the performance limitations that are inherent to trajectory tracking schemes.

In preparation for the development that follows, we set $v_{r_i}(t) = v_L(\gamma_i(t), t) + \tilde{v}_{r_i}(t)$, where $v_L(\gamma_i, t)$ is a nominal predetermined speed profile and $\tilde{v}_{r_i}$ can be seen as a perturbation component of v_{r_i} about v_L. Later, it will be shown that $v_L(.,.)$ is common to all the vehicles and known in advance and that

$$(2.4) \qquad \tilde{v}_{r_i}(t) := v_{r_i}(t) - v_L(\gamma_i(t), t)$$

(the remaining component of $v_{r_i}(t)$) is not known beforehand. We assume that $y_{d_i}(.)$ is sufficiently smooth with respect to its argument. We further assume that $v_L(.,.)$ is bounded and globally Lipschitz with respect to the first argument, that is, $\exists\, v_M, l > 0$, such that $|v_L(\gamma_i, t)| \leq v_M$ and $|v_L(\gamma_i, t) - v_L(\gamma_j, t)| \leq l|\gamma_i - \gamma_j|$.

Consider vehicle i and assume a feedback control law $u_i = u_i(x_i, y_{d_i}, v_L)$ exists that solves the PF problem of Definition 2.1. Let the corresponding closed-loop PF system be described by

$$(2.5) \qquad \dot{\zeta}_i = f_{c_i}(t, \zeta_i, \tilde{v}_{r_i}, d_i),$$

where d_i subsumes all the exogenous inputs (including disturbances and measurement noises), $\tilde{v}_{r_i}$ is defined as in (2.4), and state vector ζ_i includes necessarily e_i but may or may not include η_i. Two types of PF strategies will be considered:

1. *Type* I. In this strategy, variable η_i plays the role of an auxiliary state for the PF algorithm and specifies the evolution of γ_i. In this case η_i is a state of the closed-loop PF system, that is, ζ_i includes η_i.
2. *Type* II. This strategy is equivalent to making $\eta_i = 0$. The dynamics of $\dot{\gamma}_i$ are simply $\dot{\gamma}_i = v_{r_i}$. Clearly, in this case ζ_i does not include η_i.

We now recall the definitions of input-to-state stable (ISS) and input-to-state practical stable (ISpS) for a dynamical system. See [59] and [31, p. 217] for details on ISS and ISpS and their relation to Lyapunov theory. System (2.5) is said to be

ISpS if there exist a class $\mathcal{KL}$ function $\beta(.,.)$, class $\mathcal{K}$ functions[1] $\rho_i(.)$; $i = 1, 2$, and a constant $\rho_3 > 0$ such that for any inputs $\tilde{v}_{r_i}$ and d_i and any initial condition $\zeta_i(t_0)$, the solution of (2.5) satisfies

$$\|\zeta_i(t)\| \le \beta(\|\zeta_i(t_0)\|, t-t_0) + \rho_1\left(\sup_{t_0 \le s \le t} \|\tilde{v}_{r_i}(s)\|\right) + \rho_2\left(\sup_{t_0 \le s \le t} \|d_i(s)\|\right) + \rho_3 \quad \forall t \ge t_0.$$

System (2.5) is said to be ISS if it satisfies the conditions of ISpS with $\rho_3 = 0$.

ASSUMPTION 2.2. *We assume there exists a Lyapunov function $W_i(t, \zeta_i)$ for (2.5) satisfying*

$$(2.6) \qquad\qquad \underline{\alpha}_1 \|\zeta_i\|^2 \le W_i \le \bar{\alpha}_1 \|\zeta_i\|^2,$$

$$(2.7) \qquad\qquad \dot{W}_i \le -\lambda_1 W_i + \rho_1 |\tilde{v}_{r_i}|^2 + \rho_2 d_i^2,$$

where λ_1, ρ_1, ρ_2, $\underline{\alpha}_1$, and $\bar{\alpha}_1$ are positive values and $\dot{W}_i$ is computed along the solutions of (2.5), that is,

$$\dot{W}_i = \frac{\partial W_i}{\partial t} + \frac{\partial W_i}{\partial \zeta_i} f_{c_i}.$$

With this assumption, the closed-loop PF system (2.5) is ISS with input $(d_i, \tilde{v}_{r_i})$ and state ζ_i. To verify this, integrate (2.7) and use (2.6) to obtain

$$\underline{\alpha}_1 \|\zeta_i(t)\|^2 \le \bar{\alpha}_1 \|\zeta_i(t_0)\|^2 e^{-\lambda_1(t-t_0)} + \frac{\rho_1}{\lambda_1} \sup |\tilde{v}_{r_i}|^2 + \frac{\rho_2}{\lambda_1} \sup |d_i|^2,$$

and therefore

$$\|\zeta_i(t)\| \le \alpha \|\zeta_i(t_0)\| e^{-0.5\lambda_1(t-t_0)} + \rho_v \sup |\tilde{v}_{r_i}| + \rho_d \sup |d_i|,$$

with $\alpha = \sqrt{\bar{\alpha}_1/\underline{\alpha}_1}$, $\rho_v = \sqrt{\rho_1/(\lambda_1\underline{\alpha}_1)}$, and $\rho_d = \rho_2/(\lambda_1\underline{\alpha}_1)$.

Assuming a PF controller has been implemented for each vehicle, it now remains to coordinate (that is, synchronize) the entire group of vehicles so as to achieve a desired formation pattern compatible with the paths adopted. As will become clear, this will be achieved by adjusting the desired speeds of the vehicles as functions of the "along-path" distances among them. To better grasp the key ideas involved in the computation of these distances, consider as a simple example the case of a fleet of vehicles that are required to move along parallel straight lines and keep themselves aligned along a direction perpendicular to the lines. See Figure 1 for the case of two vehicles.

Let Γ_i denote the desired path to be followed by vehicle i and assume Γ_i is simply parameterized by s_i, the path length. In other words, $\gamma_i = s_i$. Because each vehicle approaches the path as close as required, that is, because $y_i(t)$ becomes arbitrarily close to to $y_{d_i}(\gamma_i)$, it follows that the vehicles are (asymptotically) synchronized if $\gamma_{ij}(t) := \gamma_i(t) - \gamma_j(t) \to 0 \ \forall i, j \in \mathcal{N} := \{1, \ldots, n\}$. This shows that in the case of translated straight lines $\gamma_{i,j} = s_i - s_j$ is a good measure of the along-path distances among the vehicles. Similarly, in the case of vehicles that must be aligned along the radii of nested circumferences as in Figure 2, an appropriate measure of the distances among the vehicles is angle $\gamma_i = s_i/R_i$ where s_i denotes path length and

---

[1]A function ρ is of class $\mathcal{K}$ if it is strictly increasing and $\rho(0) = 0$. A function $\beta(r, s)$ belongs to class $\mathcal{KL}$ if the mapping $\beta(r, s)$ is of class $\mathcal{K}$ for a fixed s, is decreasing with respect to s for a fixed r, and $\beta(r, s) \to 0$ as $t \to \infty$.
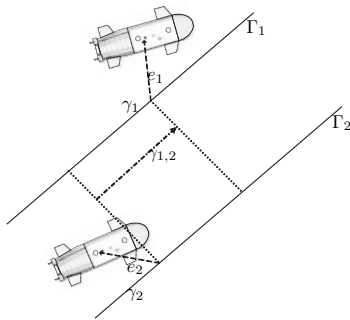
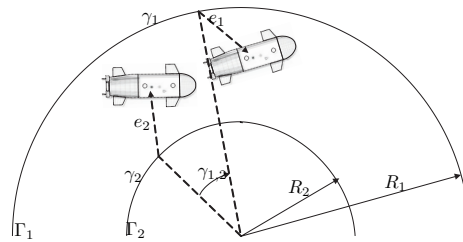FIG. 1. *Along-path distances: straight lines.*

FIG. 2. *Along-path distances: circumferences.*

R_i is the radius of circumference i. Clearly, this corresponds to adopting different parameterizations for the paths that correspond to normalizing their lengths. In both cases, we say that the vehicles are coordinated if the corresponding along-path distance is zero, that is, $\gamma_i - \gamma_j = 0$. Coordination is achieved by adjusting the desired speed of each vehicle i as a function of the along-path distances γ_{ij}; $j \in N_i$, where N_i denotes the set of vehicles with which vehicle i communicates. For arbitrary types of paths and coordination patterns, an adequate choice of path parameterizations will allow for the conclusion that the vehicles are *coordinated* or, in equivalent terms, are *synchronized*/have reached *agreement*, iff $\gamma_{i,j} = 0 \ \forall j, i \in \mathcal{N}$; see [22], [16]. Since the objective of the coordination is to coordinate variables γ_i, we will refer to them as *coordination states*.

We will require that the formation as a whole (group of multiple vehicles) travel at an assigned speed profile $v_L(\gamma_i, t)$ when coordinated, that is, $\dot{\gamma}_i = v_L \ \forall i \in \mathcal{N}$, where v_L is allowed to be a function of path parameter γ and time t. This follows from the fact that $v_L(\gamma_i, t) = v_L(\gamma_j, t)$ when $\gamma_i = \gamma_j$. This issue requires clarification. Note that the desired speed assignment is given in terms of the time derivatives of the coordination states γ_i, not in terms of the inertial speeds (actual time derivative of the positions) of the vehicles undergoing synchronization. In the limit, as shown later, the combined PF and coordination algorithms will ensure that the coordination states will be equal and the vehicle speeds will naturally approach $\frac{ds_i}{dt}$: $i \in \mathcal{N}$, so that $\frac{d\gamma_i}{dt} = \frac{d\gamma_i}{ds_i} \frac{ds_i}{dt} = v_L$. Thus, $\frac{ds_i}{dt} = v_L / \frac{d\gamma_i}{ds_i}$ which shows clearly how coordination states speed and inertial speeds depend on the path parameterizations adopted. In the case of the circumferences above, the latter relationship yields simply $\frac{ds_i}{dt} = R_i v_L$. Notice how the speed assignment in terms of the coordination states avoids the need to specify the actual inertial speeds of the vehicles in an inertial reference frame, which would be quite cumbersome. Instead, all that is required is to specify the speeds of the coordination states which are equal and degenerate simply into v_L.

From (2.3), the evolution of the coordination state γ_i, $i \in \mathcal{N}$, is governed by

$$(2.8) \qquad \dot{\gamma}_i(t) = v_{r_i}(t) + \eta_i(t),$$

where the speed tracking errors η_i are viewed as disturbance-like input signals and the speed profiles v_{r_i} are taken as control signals that must be assigned to yield coordination of the states γ_i. To achieve this objective, information is exchanged through an intervehicle communication network. Typically, all-to-all communications are impossible to achieve. In general, $\dot{\gamma}_i$ will be a function of γ_i and of the coordi-

nation states of the so-called neighboring agents defined by set N_i. For simplicity of presentation, throughout this paper we assume that the communication links are bidirectional, that is, $i \in N_j \Leftrightarrow j \in N_i$. Equipped with the above notation, we are now ready to formulate the CPF problem.

DEFINITION 2.3 (CPF). *Consider a set of vehicles V_i; $i \in \mathcal{N}$, with dynamics (2.1), together with a corresponding set of paths $y_{d_i}(\gamma_i)$ parameterized by γ_i and a formation speed assignment $v_L(\gamma_i, t)$. Assume that for each vehicle there is a feedback control law $u_i(x_i, y_{d_i}, v_L)$ such that the closed-loop systems (2.5) satisfy Assumption 2.2. Further assume that γ_i and γ_j, $j \in N_i$, are available to vehicle $i \in \mathcal{N}$. Given $\epsilon > 0$ arbitrarily small, derive a control law for v_{r_i} such that the PF errors $\|e_i\|$, the coordination errors $\gamma_i - \gamma_j$, and the formation speed tracking errors $\dot{\gamma}_i - v_L$ $\forall i, j \in \mathcal{N}$, converge to a ball of radius ϵ around zero as $t \to \infty$.*

3. Preliminaries and basic results. With the setup adopted, graph theory becomes the tool par excellence for modeling the constraints imposed by the communication topology among the vehicles, as embodied in the definition of sets N_i, $i \in \mathcal{N}$. We now recall some key concepts from algebraic graph theory [24] and agreement algorithms and derive some basic tools that will be used in what follows.

3.1. Graph theory. Let $\mathcal{G}(\mathcal{V}, \mathcal{E})$ (abbreviated $\mathcal{G}$) be the undirected graph induced by the intervehicle communication network, with $\mathcal{V}$ denoting the set of n nodes (each corresponding to a vehicle) and $\mathcal{E}$ the set of edges (each representing a data link). Nodes i and j are said to be adjacent if there is an edge between them. A path of length r between node i and node j consists of $r + 1$ consecutive adjacent nodes. We say that $\mathcal{G}$ is connected when there exists a path connecting every two nodes in the graph. The adjacency matrix of a graph, denoted A, is a square matrix with rows and columns indexed by the nodes such that the i, j-entry of A is 1 if $j \in N_i$ and zero otherwise. The degree matrix D of a graph $\mathcal{G}$ is a diagonal matrix where the i, i-entry equals $|N_i|$, the cardinality of N_i. The Laplacian of a graph is defined as $L := D - A$. It is well known that L is symmetric and $L\mathbf{1} = \mathbf{0}$, where $\mathbf{1} := [1]_{n \times 1}$ and $\mathbf{0} := [0]_{n \times 1}$. If $\mathcal{G}$ is connected, then L has a simple eigenvalue at zero with an associated eigenvector $\mathbf{1}$, and the remaining eigenvalues are all positive.

We will be dealing with situations where the communication links are time-varying in the sense that links can appear and disappear (switch) due to intermittent failures and/or communication links scheduling. The mathematical setup required is described next.

A *complete graph* is a graph with an edge between each pair of nodes. A complete graph with n nodes has $\bar{n} = n(n-1)/2$ edges. Let $\mathcal{G}$ be a complete graph with edges numbered $1, \ldots, \bar{n}$. Consider a communication network among n agents. To model the underlying switching communication graph, let $p = [p_i]_{\bar{n} \times 1}$, where each $p_i(t) : [0, \infty) \to \{0, 1\}$ is a piecewise-continuous time-varying binary function which indicates the existence of edge i in the graph $\mathcal{G}$ at time t. Therefore, given a switching signal $p(t)$, the dynamic communication graph $\mathcal{G}_{p(t)}$ is the pair $(\mathcal{V}, \mathcal{E}_{p(t)})$, where $p_i(t) = 1$ if $i \in \mathcal{E}_{p(t)}$ and $p_i(t) = 0$ otherwise. For example, $p(t) = [1, 0, \ldots, 0]^T$ means that at time t only link number 1 is active. Denote by L_p the explicit dependence of the graph Laplacian on p and likewise for the degree matrix D_p and the adjacency matrix A_p. Further let $N_{i,p(t)}$ denote the set of the neighbors of agent i at time t.

We discard infinitely fast switchings. Formally, we let S_{dwell} denote the class of piecewise constant switching signals such that any consecutive discontinuities are separated by no less than some fixed positive constant time τ_D, the dwell time. We assume that $p(t) \in S_{dwell}$.

3.2. Brief connectivity losses (BCL). Consider the situation where the communication network changes in time so as to make the underlying dynamic communication graph $\mathcal{G}_{p(t)}$ alternately connected and disconnected. To study the impact of temporary connectivity losses on the performance of the coordination algorithms developed, we explore the concept of "brief instabilities" developed in [25]. In particular, this concept will be instrumental in capturing the percentage of time that the communication graph is not connected.

Recall that the binary value of the element p_i in p declares the existence of edge i in graph $\mathcal{G}_p$. We can thus build $2^{\bar{n}}$ graphs indexed by the different possible occurrence of vector p. Let P denote the set of all possible vectors p, and let P_c and P_{dc} denote the partitions of P that give rise to connected graphs and disconnected graphs, respectively. That is, if $p \in P_c$, then $\mathcal{G}_p$ is connected, or otherwise disconnected. Define the characteristic function of the switching signal p as

$$(3.1) \qquad \chi(p) := \left\{ \begin{array}{ll} 0, & p \in P_c, \\ 1, & p \in P_{dc}. \end{array} \right.$$

For a given time-varying $p(t) \in S_{dwell}$, the connectivity loss time $T_p(\tau, t)$ over $[\tau, t]$ is defined as

$$(3.2) \qquad T_p(t, \tau) := \int_\tau^t \chi(p(s)) ds.$$

DEFINITION 3.1 (BCL). *The communication network is said to have* BCL *if*

$$(3.3) \qquad T_p(t, \tau) \leq \alpha(t - \tau) + (1 - \alpha) T_0 \quad \forall t \geq \tau \geq 0$$

for some $T_0 > 0$ and $0 \leq \alpha \leq 1$. In this case, $p(t) \in \mathcal{P}_{BCL}(\alpha, T_0) \subset S_{dwell}$, where $\mathcal{P}_{BCL}(\alpha, T_0)$ is identified with the set of time-varying graphs for which the connectivity loss time $T_p(\tau, t)$ satisfies (3.3).

In (3.3), α provides an asymptotic upper bound on the ratio $T_p(\tau, t)/(t - \tau)$ as $t - \tau \to \infty$ and is therefore called the *asymptotic connectivity loss rate*. When $p \in P_{dc}$ over an interval $[\tau, t]$, we have $T_p(\tau, t) = t - \tau$, and the above inequality requires that $t - \tau \leq T_0$. This justifies calling T_0 the *connectivity loss upper bound*. Notice that $\alpha = 1$ means that the communications graph is never connected.

We now introduce a special coordination error vector and some preliminary results that will play an important role in the sections that follow. As will be shown later, the error state thus introduced will be zero iff the coordination states are equal. To this effect, start by stacking the coordination states in a vector $\gamma := [\gamma_i]_{n \times 1}$. Given a diagonal matrix $K > 0$, define $\beta := K^{-1} \mathbf{1}$ and the error vector

$$(3.4) \qquad \tilde{\gamma} := \mathcal{L}_\beta \gamma,$$

where

$$(3.5) \qquad \mathcal{L}_\beta := I - \frac{1}{\beta^T \mathbf{1}} \mathbf{1} \beta^T$$

and I is an identity matrix. The following lemma holds true.

LEMMA 3.2. *The error vector $\tilde{\gamma}$, the matrix $\mathcal{L}_\beta$, and the graph Laplacian L_p satisfy the following properties:*
1. *$\mathcal{L}_\beta$ has $n - 1$ eigenvalues at 1 and a single eigenvalue at 0 with right and left eigenvectors $\mathbf{1}$ and β, respectively, such that $\mathcal{L}_\beta \mathbf{1} = \mathbf{0}$ and $\beta^T \mathcal{L}_\beta = \mathbf{0}^T$.*
2. *$\mathcal{L}_\beta K L_p = K L_p \ \forall p \in P_c \cup P_{dc}$.*

3. $\nu \mathcal{L}_\beta^T K^{-1} \mathcal{L}_\beta \nu \leq \nu K^{-1} \nu \ \forall \nu \in \mathbb{R}^n$.
4. $\tilde{\gamma} = \mathbf{0} \Leftrightarrow \gamma \in \text{span}\{\mathbf{1}\}$.
5. $\beta^T \tilde{\gamma} = 0$.
6. $L_p \tilde{\gamma} = L_p \gamma \ \forall p \in P_c \cup P_{dc}$.
7. If $\|\tilde{\gamma}\| < \epsilon$, then $|\gamma_i - \gamma_j| < \sqrt{2}\epsilon$ and $\|K L_p \gamma\| < n\epsilon\|K\|$.
8. Let

$$\lambda_{2,m} := \min_{\substack{p \in P_c \\ \mathbf{1}^T \nu = 0 \\ \nu^T \nu \neq 0}} \frac{\nu^T L_p \nu}{\nu^T \nu}, \qquad \lambda_m := \min_{\substack{p \in P_c \\ \beta^T \nu = 0 \\ \nu^T \nu \neq 0}} \frac{\nu^T L_p \nu}{\nu^T \nu}, \qquad \bar{\lambda}_m := \min_{\substack{p \in P_c \cup P_{dc} \\ L_p \nu \neq 0 \\ \nu^T \nu \neq 0}} \frac{\nu^T L_p \nu}{\nu^T \nu}.$$

Then, $\lambda_m = \frac{(\beta^T \mathbf{1})^2}{n \beta^T \beta} \lambda_{2,m} > 0$ and $\bar{\lambda}_m > 0$.
9. If $z = L_{p(t)} \gamma$, then the ith component of z is $z_i = \sum_{j \in N_{i,p(t)}} \gamma_i - \gamma_j$.
10. $\|\mathcal{L}_\beta \mathbf{v}_L(\gamma, t)\| \leq \sqrt{n} \min(2 v_M, \sqrt{2}\, l \|\tilde{\gamma}\|)$, where $\mathbf{v}_L(\gamma, t) = [v_L(\gamma_i, t)]_{n \times 1}$.

Proof. See the appendix. □

Property 4 allows for the conclusion that if $\tilde{\gamma}$ tends to zero, then $|\gamma_i - \gamma_j| \to 0$ $\forall i, j \in \mathcal{N}$, as $t \to \infty$ and coordination is achieved. Property 7 gives a bound on the coordination errors $\gamma_i - \gamma_j$ given a bound on the error vector $\tilde{\gamma}$. In the literature, the connectivity of a graph with Laplacian L is defined as the second smallest eigenvalue λ_2 of L. The term $\lambda_{2,m}$ defined in property 8 is an extension of the concept of connectivity in a collective sense, defined as the smallest graph connectivity over all connected graphs $\mathcal{G}_p$. Given λ_m, the lower bound estimate $\tilde{\gamma}^T L_p \tilde{\gamma} \geq \lambda_m \tilde{\gamma}^T \tilde{\gamma}$, when $p \in P_c$, applies. An identical interpretation applies to $\bar{\lambda}_m$. Notice from property 9 that if the control signal of vehicle i is computed as a function of z_i, then the proposed control law meets the communication constraints embodied in the sets N_i.

3.3. Uniformly connected in mean topology. In the previous situation, we considered the case where the communication graph changes in time, alternating between connected and disconnected graphs. We now address a more general case where the communication graph may even fail to be connected at any instant of time; however, we assume there is a finite time $T > 0$ such that over any interval of length T the union of the different graphs is somehow connected. This statement is made precise in what follows. We now present some key results for the time-varying communication graph that borrow from [37], [38], [40].

Let $\mathcal{G}_i$, $i = 1, \ldots, q$, be q graphs defined on n nodes and denote by L_i their corresponding graph Laplacians. Define the *union graph* $\mathcal{G} = \cup_i \mathcal{G}_i$ as the graph whose edges are obtained from the union of the edges $\mathcal{E}_i$ of $\mathcal{G}_i$, $i = 1, \ldots, q$. If $\mathcal{G}$ is connected, $L = \sum_i L_i$ has a single eigenvalue at 0 with eigenvector $\mathbf{1}$. Notice that L is not necessarily the Laplacian of $\mathcal{G}$, because for an edge e, if $e \in \mathcal{E}_i$ and $e \in \mathcal{E}_j$ for $i \neq j$, then e is counted twice in L through $L_i + L_j$, while we consider only one link in $\mathcal{G}$ as representative of e. However, L has the same rank properties as the Laplacian of $\mathcal{G}$. Since $p \in S_{dwell}$ (only a finite number of switchings are allowed over any bounded time interval), the union graph is defined over time intervals in the obvious manner. Formally, given two real numbers $0 \leq t_1 \leq t_2$, the union graph $\mathcal{G}([t_1, t_2))$ is the graph whose edges are obtained from the union of the edges $\mathcal{E}_{p(t)}$ of graph $\mathcal{G}_{p(t)}$ for $t \in [t_1, t_2)$.

DEFINITION 3.3 (uniformly connected in mean (UCM)). *A switching communication graph $\mathcal{G}_{p(t)}$ is UCM if there exists $T > 0$ such that for every $t \geq 0$ the union graph $\mathcal{G}([t, t + T))$ is connected.*

For a given $t > 0$, let $s_0 = t$ and the sequence s_i, $i = 1, \ldots, q$, be the time instants at which switching happens over the interval $[t, t+T)$. If the switching communication graph is UCM, then the union graph $\cup_{i=0}^{q} \mathcal{G}_i$ is connected and $\sum_{i=0}^{q} L_{p(s_i)}$ has a single eigenvalue at origin with eigenvector $\mathbf{1}$.

Consider the linear time-varying system

$$(3.6) \qquad\qquad\qquad \dot{\gamma} = -K L_p \gamma,$$

where K is a positive definite diagonal matrix and L_p is the Laplacian matrix of a dynamic graph $\mathcal{G}_p$. The following theorem holds; see, for example, [38].

THEOREM 3.4 (agreement). *Coordination (agreement) among the variables γ_i with dynamics (3.6) is achieved uniformly exponentially if the switching communication graph $\mathcal{G}_{p(t)}$ is UCM. That is, under this connectivity condition, all the coordination errors $\gamma_{ij}(t)$ converge to zero and $\dot{\gamma}_i \to 0$ as $t \to \infty$.*

We now consider the delayed version of (3.6). Let the coordination states γ_i evolve according to

$$(3.7) \qquad\qquad \dot{\gamma}(t) = -K D_{p(t)} \gamma(t) + K A_{p(t)} \gamma(t - \tau),$$

where $D_{p(t)}$ and $A_{p(t)}$ are the degree matrix and the adjacency matrix of $\mathcal{G}_{p(t)}$, respectively. The following theorem can be derived from the results in [40].

THEOREM 3.5 (agreement-delayed information). *The variables γ_i with dynamics (3.7) agree uniformly exponentially for $\tau \geq 0$ if the switching communication graph $\mathcal{G}_{p(t)}$ is UCM, that is, under this connectivity condition, all the coordination states $\gamma_i(t)$ converge to the same value and $\dot{\gamma}_i \to 0$ as $t \to \infty$.*

A version of Definition 3.3 for directed graphs was first introduced in [38], where the term "uniformly quasi-strongly connected" was used. Here, we adapt this definition to undirected graphs, thus the term "uniformly connected in mean" seems to be more adequate. It is interesting to point out that Theorem 3.4 follows naturally from the work in [38] or from Theorem 3.4 in [37], which recovers some of the results in [38] for linear systems. Theorem 3.4 can also be derived from Theorem 1 in [40] by using the fact that $p(t) \in S_{dwell}$ with a dwell time $\tau_D > 0$. Finally, Theorem 3.5 can be derived from Theorem 2 in [40] by noticing that $-K L_p$ is a matrix with nonnegative off-diagonal elements (Metzler matrix) with all its row-sums equal to zero.

4. System interconnections. Systems with brief instabilities. This section introduces a lemma that will be instrumental in deriving the performance measure (error decay rate) associated with the coordination algorithm that will be later derived for multivehicle systems communicating over networks with BCLs (Definition 3.1). Here, we avail ourselves of some important results on brief instabilities [25]. We start with basic definitions. A switching linear system $S : \dot{x} = A_p x + B_p u$ is a dynamical system, where A_p and B_p are functions of some time-varying vector function $p(t)$. The characteristic function of S, denoted χ, is defined as $\chi(p) = 0$ if S is stable and as $\chi(p) = 1$ otherwise. Let the instability time $T_p(t, \tau)$ of S be defined in a manner similar to (3.2). Then, S is said to have *brief instabilities* with instability bound T_0 and asymptotic instability rate α if T_p satisfies (3.3).

LEMMA 4.1 (system interconnection and brief instabilities). *Consider the coupled system consisting of two subsystems*

$$\dot{z}_1 = \phi_1(t, z_1, z_2, u_1),$$
$$\dot{z}_2 = \phi_2(t, z_1, z_2, u_2),$$

denoted System 1 and System 2, respectively, where z_1 and z_2 denote the state vectors and u_1 and u_2 the inputs. Assume there exist Lyapunov functions $V_1(t, z_1)$ and $V_2(t, z_2)$ satisfying

(4.1)
$$\underline{\alpha}_1 \|z_1\|^2 \leq V_1 \leq \bar{\alpha}_1 \|z_1\|^2,$$
$$\underline{\alpha}_2 \|z_2\|^2 \leq V_2 \leq \bar{\alpha}_2 \|z_2\|^2$$

and

(4.2)
$$\frac{\partial V_1}{\partial t} + \frac{\partial V_1}{\partial z_1} \phi_1 \leq -\lambda_1 V_1 + \rho_1 \|z_2\|^2 + u_1^2,$$
$$\frac{\partial V_2}{\partial t} + \frac{\partial V_2}{\partial z_2} \phi_2 \leq -\lambda_2(t) V_2 + \rho_2 \|z_1\|^2 + u_2^2,$$

where $\underline{\alpha}_i$, $\bar{\alpha}_i$, ρ_i, $i = 1, 2$, and λ_1 are positive values. Let system 2 have brief instabilities characterized by

(4.3)
$$\chi(p(t)) = \begin{cases} 0, & \lambda_2(p(t)) = \lambda_2, \\ 1, & \lambda_2(p(t)) = -\tilde{\lambda}_2, \end{cases}$$

where $\lambda_2 > 0$, $\tilde{\lambda}_2 \geq 0$, with asymptotic instability rate α and instability bound T_0. Define

(4.4)
$$\lambda_0 := \frac{1}{2}(\lambda_1 + \lambda_2) - \sqrt{\frac{1}{4}(\lambda_1 + \lambda_2)^2 - \lambda_1 \lambda_2 + \frac{\rho_1 \rho_2}{\underline{\alpha}_1 \underline{\alpha}_2}}$$

that satisfies

$$\min(\lambda_1, \lambda_2) - \sqrt{\frac{\rho_1 \rho_2}{\underline{\alpha}_1 \underline{\alpha}_2}} \leq \lambda_0 \leq \max(\lambda_1, \lambda_2) - \sqrt{\frac{\rho_1 \rho_2}{\underline{\alpha}_1 \underline{\alpha}_2}}.$$

Assume that $\alpha < \lambda_0/(\lambda_2 + \tilde{\lambda}_2)$ and

(4.5)
$$\rho_1 \rho_2 < \underline{\alpha}_1 \underline{\alpha}_2 \lambda_1 \lambda_2.$$

Then,
1. the interconnected system is ISS with respect to state $z = \mathrm{col}(z_1, z_2)$ and input $u = \mathrm{col}(u_1, u_2)$.
2. there is a Lyapunov function $V(t, z)$ such that

(4.6)
$$\underline{\alpha} \|z\|^2 \leq V \leq \bar{\alpha} \|z\|^2,$$
$$V(t) \leq cV(t_0)e^{-\lambda(t-t_0)} + g \sup_{[t_0, t]} u^2,$$

where $c = e^{(\lambda_2 + \tilde{\lambda}_2)(1-\alpha)T_0}$, $g = \frac{c}{\lambda} \max(1, \underline{\alpha}_1 (\lambda_1 - \lambda_0)/\rho_2)$, and the rate of convergence λ is given by $\lambda = \lambda_0 - \alpha(\lambda_2 + \tilde{\lambda}_2)$.

In particular, if $\rho_2 = 0$ and $\rho_1 > 0$, then the interconnected system takes a cascade form and is ISS with input u and state z. Furthermore, the system exhibits convergence rate $\lambda = \min(\lambda_1, (1 - \alpha)\lambda_2 - \alpha\tilde{\lambda}_2)$. The conclusions are also valid with $\alpha = 0$ for the case where system 2 has no instabilities, that is, $\lambda_2(t) = \lambda_2$.

   Proof. An indication of the proof for the case where ρ_1 and ρ_2 are nonzero is given next. See the appendix for the proof in the general case.

Define $V = V_1 + aV_2$ for some $a > 0$ to be chosen later. Taking the derivative of V yields

$$\dot{V} \leq -\left(\lambda_1 - \frac{a\rho_2}{\underline{\alpha}_1}\right)V_1 - a\left(\lambda_2(t) - \frac{\rho_1}{a\underline{\alpha}_2}\right)V_2 + g\|d\|^2,$$

where $g = \max(1, a)$. Given any constant $\lambda_2 > 0$, there exists $a > 0$ such that

(4.7) $$\lambda_1 - \frac{a\rho_2}{\underline{\alpha}_1} = \lambda_2 - \frac{\rho_1}{a\underline{\alpha}_2}$$

if (4.5) is satisfied (small-gain condition). Then $\dot{V} \leq -\lambda_0 V + g\|d\|^2$, where λ_0 is given by (4.4), and the interconnected system is ISS with input d. Furthermore, its convergence rate is $\lambda = \lambda_0$.

Consider now the situation where $\lambda_2(t)$ is time-varying. In this case, $\dot{V} \leq -\lambda_0 V + a(\lambda_2 - \lambda_2(t))V_2 + g\|d\|$. Because system 2 has brief instabilities with characteristic function $\chi(p)$, using the relationship $aV_2 = V - V_1$ yields

$$\dot{V} \leq -(\lambda_0 - \lambda_3\chi(p(t)))V + g\|d\|^2,$$

where $\lambda_3 := \lambda_2 + \tilde{\lambda}_2$. Integrating the above differential inequalities, it can be shown that

$$V(t) \leq V(t_0)e^{-\lambda_0(t-t_0)+\lambda_3 T_p} + g\sup_{[t_0,t]}\|d\|^2\int_{t_0}^t e^{-\lambda_0(t-\tau)+\lambda_3 T_p}d\tau.$$

Using (3.3) concludes the proof. □

It is interesting to notice how the lemma invokes two conditions: (i) the small-gain condition (4.5), which is sufficient to guarantee that the results stated hold true when system 2 is stable, and (ii) the extra inequality $\alpha < \lambda_0/(\lambda_2 + \tilde{\lambda}_2)$, that must also be satisfied when system 2 has brief instabilities. In this respect, the above lemma generalizes the results derived in [27] for the case where system 2 has no brief instabilities. As an example of application of the lemma, assume $\lambda_1 = \lambda_2 = \tilde{\lambda}_2 = \frac{1}{k}\sqrt{\frac{\rho_1\rho_2}{\underline{\alpha}_1\underline{\alpha}_2}}$, where $0 < k < 1$. Then the small-gain condition is satisfied and the interconnected system of the lemma above is ISS if $\alpha < \frac{1-k}{2}$, which is smaller than 0.5 for any admissible k.

Equipped with the results derived so far, the next two sections offer solutions to the CPF problem formulated in section 2.

5. CPF in the absence of communication delays. Consider the coordination control problem introduced in section 2 with a switching communication topology parameterized by $p : [0, \infty) \to \{0, 1\}$ and with no communication delays. Recall that the coordination states γ_i are governed by (2.8). Inspired by the work in [28], [61], we propose the following decentralized feedback law for the reference speeds v_{r_i} as a function of the information obtained from the neighboring vehicles:

(5.1) $$v_{r_i} = v_L - k_i \sum_{j \in N_{i,p(t)}} (\gamma_i(t) - \gamma_j(t)),$$

where $v_L(\gamma_i, t)$ is the common, nominal speed assigned to the fleet of vehicles and $k_i > 0$. Let $k_m := \min_i k_i$ and $k_M := \max_i k_i$. Notice that with this choice of control law, the term $\tilde{v}_{r_i} = v_{r_i} - v_L$, for which the time derivative is not available, is given by

(5.2) $$\tilde{v}_{r_i} = -k_i \sum_{j \in N_{i,p(t)}} (\gamma_i(t) - \gamma_j(t)).$$

Using (2.8), (5.1), and property 9 of Lemma 3.2, the coordination control closed-loop system can be written in vector form as

$$\dot{\gamma} = -KL_{p(t)}\gamma + \mathbf{v}_L(\gamma, t) + g_\eta\eta, \tag{5.3}$$

where $K = \text{diag}[k_i]$. The auxiliary term g_η was added for simplicity of exposition: $g_\eta = 1$ when the closed-loop PF system is of Type I (η is considered a state), and $g_\eta = 0$ when the PF system is of Type II ($\eta = \mathbf{0}$); see Assumption 2.2. Using properties 2 and 6 of Lemma 3.2, the coordination dynamics (5.3) take the form

$$\dot{\tilde{\gamma}} = -KL_p\tilde{\gamma} + \mathcal{L}_\beta\mathbf{v}_L(\gamma, t) + g_\eta\mathcal{L}_\beta\eta. \tag{5.4}$$

Notice from (5.3) that η can be viewed as a coupling term from the PF to the coordination dynamics.

At this stage, in preparation for the following sections, we state a lemma on an ISS property that applies to a collection of PF systems.

LEMMA 5.1. *Consider n PF subsystems, each satisfying Assumption 2.2, and let* $\zeta = [\zeta_i]_{n\times 1}$. *Then there exists a single Lyapunov function* V_1 *satisfying*

$$\underline{\alpha}_1\|\zeta\|^2 \leq V_1 \leq \bar{\alpha}_1\|\zeta\|^2, \tag{5.5}$$
$$\dot{V}_1 \leq -\lambda_1 V_1 + \rho_1 n^2 k_M^2\|\tilde{\gamma}\|^2 + u_1^2,$$

where $u_1^2 := \sum_{i=1}^n d_i^2$. *In addition, the ISS property*

$$\|\eta(t)\| \leq \|\zeta(t)\| \leq e^{-\bar{\lambda}_1(t-t_0)}\|\zeta(t_0)\| + \bar{\rho}_1 \sup_{\tau\in[t_0,t)}\|\tilde{\gamma}\| + \bar{\rho}_2\|u_1\| \tag{5.6}$$

holds with $\bar{\lambda}_1 = \frac{\underline{\alpha}_1}{2\bar{\alpha}_1}\lambda_1$, $\bar{\rho}_1 = \sqrt{\frac{\rho_1 n^2 k_M^2}{\lambda_1\bar{\alpha}_1}}$, *and* $\bar{\rho}_2 = \frac{1}{\sqrt{\lambda_1\bar{\alpha}_1}}$.

Proof. See the appendix. ◻

Close inspection of the ISS property (5.6) and the dynamics (5.4) shows that the PF and coordination systems form a feedback interconnected system.

To deal with switching communication topologies, two approaches are introduced next: "uniform switching topologies" and "brief connectivity losses," as defined in section 2. We now derive conditions under which the overall closed-loop system consisting of the PF and coordination subsystems is stable. We also derive some convergence properties for the complete system.

5.1. UCM topology. This section addresses the case where the communication network changes but the underlying communication graph is UCM (see Definition 3.3). Recall in this case that there is $T > 0$ such that for any $t \geq 0$, the union graph $\mathcal{G}([t, t+T))$ is connected. The section starts with some preliminary results leading to the statement of Theorem 5.2, a proof of which is included in the appendix.

Consider the unforced coordination closed-loop dynamics derived from (5.4), that is,

$$\dot{\tilde{\gamma}} = -KL_p\tilde{\gamma}. \tag{5.7}$$

First, we will show that if the switching communication graph is UCM (with parameter $T > 0$), then $\forall t > 0$, $\exists\tau \in [t, t+T)$, such that $L_{p(\tau)}\tilde{\gamma}(\tau) \neq \mathbf{0}$. To this effect, we let $V = \frac{1}{2}\tilde{\gamma}^T K^{-1}\tilde{\gamma}$ whose time derivative along the solutions of (5.7) is

$$\dot{V} = -\tilde{\gamma}^T L_p\tilde{\gamma}.$$

Notice that $\dot{V}$ is negative semidefinite whether the graph is connected or not. Thus, $\tilde{\gamma}$ remains bounded. Consider now the sequence s_i, $i = 1, \ldots, q$, of switching times in the interval $[t, t+T)$, with $t < s_1 < s_q < t + T$ and $s_i \le s_{i+1} - \tau_D$, $i = 1, \ldots, q-1$, where τ_D is the dwell time. Let $s_0 = \min(t, s_1 - \tau_D)$ and $T_1 = \max(s_q + \tau_D, t+T) - s_0$. With this construction $T \le T_1 \le T + 2\tau_D$, $s_1 - \tau_D \ge s_0$, and $s_q + \tau_D \le s_0 + T_1$. We now show that[2] $\exists \tau \in \mathbb{T} := [s_0, s_0 + T_1)$ such that $L_{p(\tau)}\tilde{\gamma}(\tau) \ne \mathbf{0}$.

Assume by contradiction that $L_p\tilde{\gamma} = \mathbf{0}$ $\forall \tau \in \mathbb{T}$ and discard the trivial solution $\tilde{\gamma} = \mathbf{0}$. Then, from (5.7) it follows that $\dot{\tilde{\gamma}} = \mathbf{0}$; that is, $\tilde{\gamma}$ remains unchanged over $\mathbb{T}$. Therefore,

$$\mathbf{0} = \sum_{i=0}^{q} L_{p(s_i)}\tilde{\gamma}(s_i) = \left(\sum_{i=0}^{q} L_{p(s_i)}\right)\tilde{\gamma}(s_0).$$

As shown in section 3, since the graph is UCM the matrix $\sum_{i=0}^{q} L_{p(s_i)}$ has rank $n-1$ and its kernel is $\mathrm{span}\{\mathbf{1}\}$. As a consequence, $\tilde{\gamma}(s_0) \in \mathrm{span}\{\mathbf{1}\}$, which contradicts the fact that $\beta^T\tilde{\gamma} = 0$.

Without loss of generality, assume $L_{p(s_0)}\tilde{\gamma}(s_0) \ne \mathbf{0}$ and define $\mathbb{T}_D := [s_0, s_0 + \tau_D)$. Clearly, $\forall \bar{t} \in \mathbb{T}_D$ the inequality $L_{p(\bar{t})}\tilde{\gamma}(\bar{t}) \ne \mathbf{0}$ applies because (5.7) is a linear time invariant system during the interval considered and its solutions cannot tend to zero in finite time. It follows that

$$(5.8) \qquad \dot{V}(\bar{t}) \le \begin{cases} -2k_m\bar{\lambda}_m V(\bar{t}), & \bar{t} \in \mathbb{T}_D, \\ 0, & \bar{t} \in \mathbb{T}\backslash\mathbb{T}_D, \end{cases}$$

with $\bar{\lambda}_m$ as defined in property 8 of Lemma 3.2. We can now conclude that system (5.7) with UCM switching communication graphs has brief instabilities with asymptotic instability rate $\bar{\alpha} = 1 - \tau_D/T_1 \le 1 - \tau_D/(T + 2\tau_D)$ and instability upper bound $\bar{T}_0 = T_1 - \tau_D \le T + \tau_D$. That is, if a characteristic function $\bar{\chi}$ is defined as

$$\bar{\chi}(t) = \begin{cases} 0, & t \in \mathbb{T}_D, \\ 1, & t \in \mathbb{T}\backslash\mathbb{T}_D, \end{cases}$$

then $\dot{V}(t) \le -2k_m\bar{\lambda}_m(1 - \bar{\chi}(t))V(t)$. Integrating this differential inequality yields

$$V(t) \le cV(\tau)e^{-2\lambda_\alpha(t-\tau)} \quad \forall t \ge \tau \ge 0,$$

with

$$(5.9) \qquad \lambda_\alpha = (1 - \bar{\alpha})k_m\bar{\lambda}_m, \quad c = e^{2\lambda_\alpha\bar{T}_0},$$

and where we used the fact that

$$\int_t^\tau \bar{\chi}(s)ds \le \bar{\alpha}(t - \tau) + (1 - \bar{\alpha})\bar{T}_0 \quad \forall t \ge \tau \ge 0.$$

Therefore, $\|\tilde{\gamma}(t)\| \le c_1 e^{-\lambda_\alpha(t-\tau)}\|\tilde{\gamma}(\tau)\|$ and

$$(5.10) \qquad \|\Phi_p(t, \tau)\| \le c_1 e^{-\lambda_\alpha(t-\tau)},$$

where $\Phi_p(t, \tau)$ denotes the state transition matrix of (5.7) and $c_1 = \sqrt{\frac{ck_M}{k_m}}$. Notice that the above inequality is valid for all $p(t) \in S_{dwell}$ such that the graph $\mathcal{G}_p$ is UCM.

---

[2]Notice that if $\exists \tau \in \mathbb{T}$ such that $L_{p(\tau)}\tilde{\gamma}(\tau) \ne \mathbf{0}$, then $\exists \tau_1 \in [t, t+T)$ such that $L_{p(\tau_1)}\tilde{\gamma}(\tau_1) \ne \mathbf{0}$ because $t \le s_0 + \tau_D$ and $t + T \ge s_0 + T - \tau_D$.

For a given switching signal $p(t)$, input $\eta(t)$, and initial state $\gamma(t_0)$, the solution of (5.4) is given by (see [53, p. 87])

$$\tilde{\gamma}(t) = \Phi_p(t, t_0)\tilde{\gamma}(t_0) + \int_{t_0}^t \Phi_p(t, \tau)\mathcal{L}_\beta \mathbf{v}_L(\gamma(\tau), \tau)d\tau + g_\eta \int_{t_0}^t \Phi_p(t, \tau)\mathcal{L}_\beta \eta(\tau)d\tau \quad \forall t \geq t_0.$$

Letting

$$(5.11) \qquad\qquad \bar{\lambda}_\alpha = \lambda_\alpha - c_1\sqrt{2n}l = \lambda_\alpha - e^{\lambda_\alpha \bar{T}_0}l\sqrt{2n\frac{k_M}{k_m}}$$

and using (5.10) and property 10 of Lemma 3.2, an upper bound for $\tilde{\gamma}(t)$ can be derived as
(5.12)

$$\|\tilde{\gamma}(t)\| \leq c_1 e^{-\lambda_\alpha(t-t_0)}\|\tilde{\gamma}(t_0)\| + c_1 l\sqrt{2n}\int_{t_0}^t e^{-\lambda_\alpha(t-\tau)}\|\tilde{\gamma}(\tau)\|d\tau + g_\eta\frac{c_1}{\lambda_\alpha}\sup_{\tau\in[t_0,t)}\|\eta(\tau)\|$$

if $\bar{\lambda}_\alpha > 0$, and

$$(5.13) \qquad \|\tilde{\gamma}(t)\| \leq c_1 e^{-\lambda_\alpha(t-t_0)}\|\tilde{\gamma}(t_0)\| + \frac{2v_M c_1\sqrt{n}}{\lambda_\alpha} + g_\eta\frac{c_1}{\lambda_\alpha}\sup_{\tau\in[t_0,t)}\|\eta(\tau)\|$$

otherwise. It is now straightforward to multiply both sides of (5.12) by $e^{\lambda_\alpha t}$ and to use the Gronwall–Bellman theorem [31, p. 66] to arrive at

$$(5.14) \qquad \|\tilde{\gamma}(t)\| \leq c_1 e^{-\bar{\lambda}_\alpha(t-t_0)}\|\tilde{\gamma}(t_0)\| + g_\eta\frac{c_1}{\bar{\lambda}_\alpha}\sup\|\eta(\tau)\|$$

provided that $\bar{\lambda}_\alpha > 0$. Notice from (5.11) that $\bar{\lambda}_\alpha$ cannot be made arbitrarily large. It can be shown that there are control gains $(k_m = k_M)$ that make $\bar{\lambda}_\alpha > 0$ if the Lipschitz constant l of v_L satisfies

$$(5.15) \qquad\qquad l < \frac{1}{(T + \tau_D)\sqrt{2ne}}.$$

For each such l, the corresponding maximum value of $\bar{\lambda}_\alpha$ can be easily computed.

Equipped with these introductory results, we now state the main theorem of this section.

THEOREM 5.2 (CPF with UCM). *Consider the interconnected system Σ depicted in Figure* 3, *consisting of n PF subsystems satisfying Assumption* 2.2 *together with the coordination control (CC) subsystem* (5.3) *supported by a communication network*
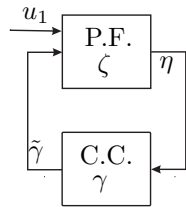

FIG. 3. Σ: *Overall closed-loop system consisting of the PF and CC subsystems.*

that is UCM with parameter T and switching dwell time τ_D. Then, Σ is input-to-state practical stable (ISpS) with respect to the states $\tilde{\gamma}$ and ζ, the input u_1, and the constant $2v_M c_1 \sqrt{n}/\lambda_\alpha$ if

$$(5.16) \qquad \begin{cases} c_1 \sqrt{\frac{\rho_1 n^2 k_M^2}{\lambda_1 \bar{\alpha}_1}} < \bar{\lambda}_0, & PF \text{ of Type I,} \\ always, & PF \text{ of Type II,} \end{cases}$$

where $\bar{\lambda}_0 = \lambda_\alpha$ as defined in (5.9). If (5.15) holds, the control gains can be chosen such that $\bar{\lambda}_\alpha > 0$. In this case, Σ is ISS with respect to the states $\tilde{\gamma}$ and ζ and input u_1 under condition (5.16) with $\bar{\lambda}_0 = \bar{\lambda}_\alpha$ as defined in (5.11). Furthermore, the PF error vectors e_i, the speed tracking errors $|\dot{\gamma}_i - v_L|$, and the coordination errors $|\gamma_i - \gamma_j|$ $\forall i, j \in \mathcal{N}$ converge exponentially fast to some ball around zero as $t \to \infty$, with rate at least $\min(\bar{\lambda}_0, \bar{\lambda}_1)$.

Proof. A proof of (5.15) is given in the appendix. Using the ISS version of the small-gain theorem for the interconnection of (5.14) and (5.6) in the case of $\bar{\lambda}_\alpha > 0$, and for the interconnection of (5.13) and (5.6) otherwise, leads to the result. □

From the above, under the UCM assumption, it follows that the complete CPF control system is ISS if condition (5.15) is satisfied. In the absence of disturbances and noise, the origin of the system becomes globally asymptotically stable (in fact, exponentially stable). In the case when condition (5.15) is not satisfied, all that can be shown is that the complete system is ISpS.

5.2. BCLs. This section addresses the situation where the communication network has BCLs; see Definition 3.1. In this case the underlying communication graph switches between connected and disconnected configurations with known asymptotic connectivity loss rate α and connectivity loss upper bound T_o.

The following result provides conditions under which the overall closed-loop system consisting of the PF and coordination subsystems is ISS.

THEOREM 5.3 (CPF with BCLs). *Consider the interconnected system Σ depicted in Figure 3, consisting of n PF subsystems that satisfy Assumption 2.2 and the coordination subsystem (5.3) with a communication network subjected to BCLs characterized by (3.3). Let $\lambda_2 := k_m \lambda_m - \frac{k_M l \sqrt{2n}}{k_m}$. Define $k_g := \frac{k_m \lambda_2^2}{n^2 k_M^3}$ and*

$$\lambda_0 = \tilde{\lambda}_0 - \sqrt{\tilde{\lambda}_0^2 - \lambda_1 \lambda_2 \left(1 - \frac{\rho_1}{k_g \underline{\alpha}_1 \lambda_1}\right)},$$

where $\tilde{\lambda}_0 = \frac{1}{2}(\lambda_1 + \lambda_2)$ and λ_m is defined in Lemma 3.2, property 8. Assume

$$(5.17) \qquad \frac{k_m^2}{k_M} > \frac{l\sqrt{2n}}{\lambda_m}.$$

Further assume the following conditions hold:

(a) [PF of Type I] *The asymptotic connectivity losses rate α satisfies*

$$\alpha < \frac{\lambda_0}{2k_m \lambda_m}$$

and

$$\frac{\rho_1}{\underline{\alpha}_1 \lambda_1} < k_g.$$

(b) [PF of Type II] $\alpha < 1 - \frac{k_M l \sqrt{2n}}{\lambda_m k_m^2}$.

Then, Σ is ISS with respect to the states $\tilde{\gamma}$ and ζ and input u_1 (see Figure 3). Furthermore, the PF error vectors e_i, the speed tracking errors $|\dot{\gamma}_i - v_L|$, and the coordination errors $|\gamma_i - \gamma_j| \; \forall i, j \in \mathcal{N}$ converge exponentially fast to some ball around zero (depending on the size of u_1) as $t \to \infty$, with rate at least

$$\lambda = \begin{cases} \lambda_0 - 2\alpha k_m \lambda_m, & \textit{PF of Type } I, \\ \min(\lambda_1, \lambda_2 - 2\alpha k_m \lambda_m), & \textit{PF of Type } II. \end{cases}$$

Proof. Choose the Lyapunov candidate function

$$V_2 := \frac{1}{2} \tilde{\gamma}^T K^{-1} \tilde{\gamma}$$

whose time derivative along the solutions of (5.4) is

$$\dot{V}_2 = -\tilde{\gamma}^T L_p \tilde{\gamma} + \tilde{\gamma}^T K^{-1} \mathcal{L}_\beta \mathbf{v}_L(\gamma, t) + g_\eta \tilde{\gamma}^T K^{-1} \mathcal{L}_\beta \eta$$

$$\leq -\tilde{\gamma}^T L_p \tilde{\gamma} + \frac{l\sqrt{2n}}{k_m} \|\tilde{\gamma}\|^2 + g_\eta \theta_1 \tilde{\gamma}^T K^{-1} \tilde{\gamma} + \frac{g_\eta}{4\theta_1} \eta^T \mathcal{L}_\beta^T K^{-1} \mathcal{L}_\beta \eta,$$

where we used Young's inequality and property 10 of Lemma 3.2. Using properties 3 and 8 of Lemma 3.2, the above inequality yields

(5.18)
$$\dot{V}_2 \leq \begin{cases} -\lambda_2 V_2 + \rho_2 \|\eta\|^2, & p \in P_c, \\ \tilde{\lambda}_2 V_2 + \rho_2 \|\eta\|^2, & p \in P_{dc}, \end{cases}$$

with $\tilde{\lambda}_2 = \frac{2k_M l \sqrt{2n}}{k_m} + 2g_\eta \theta_1$, $\lambda_2 = 2\lambda_m k_m - \tilde{\lambda}_2$, $\rho_2 = \frac{g_\eta}{4k_m \theta_1}$. In order for λ_2 and $\tilde{\lambda}_2$ to be positive, θ_1 must satisfy $0 < \theta_1 < \lambda_m k_m - \frac{l\sqrt{2n} k_M}{k_m}$. It is straightforward to check that this condition holds if $\frac{k_m^2}{k_M} > \frac{l\sqrt{2n}}{\lambda_m}$.

Close inspection of (5.5) and (5.18) shows that the PF and coordination subsystems form a feedback interconnected system with η and $\tilde{\gamma}$ as interacting signals, as shown in Figure 3. We now use Lemma 4.1 and the fact that the coordination subsystem has BCLs as defined in (3.3) to find conditions under which the interconnected system is ISS from input u_1. We consider the cases where the PF algorithms are of Type I or II.

[*PF of Type* I] Consider the feedback interconnection of (5.5) and (5.18) for the case where $g_\eta = 1$, that is, with $\rho_2 > 0$. Resorting to Lemma 4.1 for interconnected systems with brief instabilities and applying the small-gain condition (4.5), we obtain

$$(\rho_1 n^2 k_M^2) \left(\frac{1}{4k_m \theta_1} \right) < (\underline{\alpha}_1) \left(\frac{1}{2k_M} \right) (\lambda_1) \left(2\lambda_m k_m - 2\frac{l\sqrt{2n} k_M}{k_m} - 2\theta_1 \right),$$

or equivalently,

$$\frac{\rho_1}{\underline{\alpha}_1 \lambda_1} < \frac{4k_m}{n^2 k_M^3} \theta_1 \left(\lambda_m k_m - \frac{l\sqrt{2n} k_M}{k_m} - \theta_1 \right),$$

the right-hand side of which is maximized for $\theta_1 = \frac{1}{2k_m}(\lambda_m k_m^2 - l\sqrt{2n} k_M)$. Inserting the latter value of θ_1 in the inequality above, the conditions of the theorem for PF strategies of Type I follow immediately.

[*PF of Type* II] In this case the interconnection of (5.5) and (5.18) takes a cascade form, that is, $g_\eta = 0$ and (5.18) simplifies to

$$\dot{V}_2 \leq \begin{cases} -\lambda_2 V_2, & p \in P_c, \\ \tilde{\lambda}_2 V_2, & p \in P_{dc}, \end{cases}$$

where $\tilde{\lambda}_2 = 2\frac{l\sqrt{2n}k_M}{k_m}$ and $\lambda_2 = 2\lambda_m k_m - \tilde{\lambda}_2$. Using Lemma 4.1 with $\rho_2 = 0$ the conditions of the theorem for PF strategies of Type I are easily obtained. $\square$

At this point, it is interesting to work out a simple numerical example to illustrate some of the results derived. To this effect, consider the CPF problem for three vehicles ($n = 3$). In this case, $\lambda_m = 1$. We consider both the case where the speed profile v_L is constant and the case where $v_L(\gamma_i) = 2 + \sin(\gamma_i)$, for which $l = 0$ and $l = 1$, respectively. Choose $K = 2\sqrt{6}I_3$ to guarantee condition (5.17) for both cases of v_L. Further assume that the ISS property of the PF subsystem is satisfied with $\lambda_1 = \sqrt{6}$ and $\underline{\alpha}_1 = \sqrt{6}$. It is now straightforward to compute the following parameters consecutively. For $l = 0$: $\lambda_2 = 2\sqrt{6}$, $k_g = 4/36$, and $\tilde{\lambda}_0 = 3/2\sqrt{6}$. The small-gain condition (4.5) will require that $\rho_1 < 4/6$. For $l = 1$: $\lambda_2 = \sqrt{6}$, $k_g = 1/36$, and $\tilde{\lambda}_0 = \sqrt{6}$. The same small-gain condition will yield $\rho_1 < 1/6$ in this case. As expected, ρ_1 (which can be viewed as a stability margin) is reduced when the v_L depends on the path parameter. Let $\rho_1 = 1/24$ to ensure stability for both cases of v_L above. We can now compute $\lambda_0 = 0.54\sqrt{6}$ for $l = 0$ and $\lambda_0 = 0.5\sqrt{6}$ for $l = 1$. It follows from the above that when PF is of Type I the interconnected system will be ISS if the asymptotic connectivity loss rate is $\alpha < 13.5\%$ for $l = 0$ and $\alpha < 12.5\%$ for $l = 1$. When PF is of Type II, the bounds are relaxed to $\alpha < 100\%$ for $l = 0$ and $\alpha < 50\%$ for $l = 1$. Better convergence rates could be guaranteed if one were to aim for ISpS rather than ISS.

6. CPF: Delayed information. In this section we study the problem of CPF in the presence of communication delays. We consider the case where all communication channels have the same delay, $\tau > 0$. We further assume that the PF closed-loop subsystems are of Type II, that is, $\eta = \mathbf{0}$.

Motivated by (5.1), we assume that the control law for the reference speed v_{r_i} of each vehicle is given by

$$(6.1) \qquad v_{r_i} = v_L - k_i \sum_{j \in N_{i,p(t)}} (\gamma_i(t) - \gamma_j(t - \tau)).$$

Using (2.8) and (6.1), the closed-loop coordination subsystem can be written as

$$(6.2) \qquad \dot{\gamma}(t) = \mathbf{v}_L(\gamma, t) - KD_{p(t)}\gamma(t) + KA_{p(t)}\gamma(t - \tau),$$

where D_p and A_p are the degree matrix and the adjacency matrix of the communication graph, respectively. We now determine conditions under which coordination is achieved, that is, under which there exists a signal $\gamma_0(t)$ such that $\gamma = \gamma_0(t)\mathbf{1}$ is a solution of (6.2). Should such a solution exist, then substituting it in (6.2) and using the fact that $A_p = D_p - L_p$ yields

$$\dot{\gamma}_0\mathbf{1} = v_L(\gamma_0, t)\mathbf{1} - KD_p\gamma_0(t)\mathbf{1} + K(D_p - L_p)\gamma_0(t - \tau)\mathbf{1},$$

which simplifies to

$$(6.3) \qquad \dot{\gamma}_0\mathbf{1} - v_L\mathbf{1} = -(\gamma_0(t) - \gamma_0(t - \tau))KD_p\mathbf{1}.$$

The equality above is verified iff all elements of the right-hand side vector are equal. For this to be true, one of the following two conditions must apply:

[C1] $\gamma_0(t)$ is either a constant or a periodic signal with period τ. In this case $\gamma_0(t) - \gamma_0(t - \tau) = 0 \ \forall t$ and (6.3) holds with $\dot{\gamma}_0 = v_L$. This condition is not relevant from a practical standpoint.

[C2] $\forall t, \ KD_{p(t)} = kI$ for some $k > 0$. This requires that the degrees of the nodes of the switching communication graph $\mathcal{G}_p$ never vanish, that is, $|N_{i,p}| \neq 0 \ \forall t$, so that the degree matrix D_p is always nonsingular and we can set the control gains to $K = kD_p^{-1}$. In this case, the control gains become piecewise constant functions of p.

In view of the above discussion we consider only condition C2. To lift the constraint $|N_{i,p}| \neq 0$ and have the CPF algorithm be applicable to more general types of switching topologies, we will later modify the control law (6.1). In what follows, we assume v_L is constant. We start by studying the convergence properties of only the coordination dynamics in Lemmas 6.1 and 6.2 below. This is followed by the analysis of the combined PF and coordination systems in Theorem 6.3.

LEMMA 6.1. *Consider the coordination system dynamics* (2.8) *with the control law* (6.1). *Assume that* $|N_{i,p(t)}| \neq 0 \ \forall \ t$, *and let the control gains be* $k_i(t) = k/|N_{i,p(t)}|$. *Then, the states* γ_i *uniformly exponentially agree if the underlying communication graph* $\mathcal{G}_p$ *is UCM. In this situation,* $|\gamma_i - \gamma_j| \to 0$ *and* $\dot{\gamma}_i \to \dot{\gamma}_0$ *as* $t \to \infty$, *where* γ_0 *is a solution of the delay differential equation*

$$(6.4) \qquad \dot{\gamma}_0 = -k(\gamma_0(t) - \gamma_0(t - \tau)) + v_L.$$

Proof. As explained before, with the control law (6.1) the coordination system takes the form (6.2). Let

$$(6.5) \qquad \tilde{\gamma}(t) = \gamma(t) - \gamma_0(t)\mathbf{1}$$

and substitute γ from (6.5) in (6.2) to obtain

$$(6.6) \qquad \begin{aligned} \dot{\gamma}_0(t)\mathbf{1} + \dot{\tilde{\gamma}} = {}& -K(t)D_{p(t)}\tilde{\gamma}(t) + K(t)A_{p(t)}\tilde{\gamma}(t - \tau) + \\ & -K(t)D_{p(t)}\gamma_0(t)\mathbf{1} + K(t)A_{p(t)}\gamma_0(t - \tau)\mathbf{1} + v_L\mathbf{1}, \end{aligned}$$

which simplifies to

$$(6.7) \qquad \dot{\tilde{\gamma}} = -k\tilde{\gamma}(t) + kD_p^{-1}A_p\tilde{\gamma}(t - \tau)$$

if $\gamma_0(t)$ is the solution of (6.4) and $K(t) = kD_p^{-1}$. From Theorem 3.5, states $\tilde{\gamma}_i$ in (6.7) agree uniformly exponentially. In particular, $\tilde{\gamma} \to 0$ as $t \to \infty$. Thus, from (6.5) $\gamma \to \gamma_0\mathbf{1}$, and the results follow. $\square$

In general, if v_L is not constant the delayed differential equation (6.4) has no closed form solution. However, for the particular case of v_L constant, one solution is $\gamma_0(t) = v_L^* t$, where $v_L^* = \frac{v_L}{1 + k\tau}$. Notice that due to the transmission delay τ there is a finite error in the speed tracking; that is, $\dot{\gamma}_i$ converges to v_L^* and not to v_L.

Consider now the case where there are instants of t time at which $|N_{i,p(t)}| = 0$ for some $i \in \mathcal{N}$. Notice that with the setup adopted in this paper, this condition will necessarily hold over a countable number of disjoint intervals of time, where the length of each interval is bounded above and below by T_0 and τ_D, respectively.

In this case, (6.2) can be rewritten in terms of $\tilde{\gamma}$ defined in (6.5) as

$$(6.8) \qquad \dot{\tilde{\gamma}} = -K(t)D_{p(t)}\tilde{\gamma}(t) + K(t)A_{p(t)}\tilde{\gamma}(t - \tau) + v_L^*\tau(kI - K(t)D_p)\mathbf{1}.$$

Clearly, when $\tau = 0$ agreement is achieved for any choice of positive definite K due to Theorem 3.5. However, this is not necessarily the case when $\tau \neq 0$. To see this, assume, for example, that the agreement dynamics (6.8) are at rest, that is, $\dot{\tilde{\gamma}}_i = 0$ $\forall i \in \mathcal{N}$. Then, if $|N_{i,p(t)}| = 0$ for some i and t in a given interval of time, the dynamics of the ith row of (6.8) become $\dot{\tilde{\gamma}}_i = v_L - v_L^*$. This problem can be resolved by applying different desired speeds when vehicle i has no neighbors. The solution is stated next.

LEMMA 6.2. *Consider the coordination system dynamics with control law*

$$(6.9) \qquad v_{r_i} = \begin{cases} v_L + \frac{k}{|N_{i,p}|} \sum_{j \in N_{i,p}} \gamma_i(t) - \gamma_j(t - \tau), & N_{i,p} \neq \emptyset, \\ v_L^*, & N_{i,p} = \emptyset, \end{cases}$$

where $k > 0$. Then, the states γ_i uniformly exponentially agree if the underlying communication graph $\mathcal{G}_p$ is UCM. In this case, $|\gamma_i - \gamma_j| \to 0$ and $\dot{\gamma}_i \to v_L^*$ as $t \to \infty$.

Proof. The closed-loop coordination dynamics can be expressed in vector form as

$$\dot{\gamma} = -KD_p\gamma(t) + KA_p\gamma(t - \tau) + \frac{v_L - v_L^*}{k}KD_p\mathbf{1} + v_L^*\mathbf{1}.$$

Letting $\gamma(t) = v_L^* t \mathbf{1} + \tilde{\gamma}(t)$ simplifies the closed-loop dynamics to

$$\dot{\tilde{\gamma}} = -KD_p\tilde{\gamma}(t) + KA_p\tilde{\gamma}(t - \tau).$$

Theorem 3.5 implies that $\tilde{\gamma}$ and $\dot{\tilde{\gamma}}$ will converge to the span$\{\mathbf{1}\}$ and to $\mathbf{0}$, respectively, as $t \to \infty$. This concludes the proof. $\square$

Notice that in order to implement the control law (6.9) the vehicles need to know the delay τ in order to compute v_L^*. This raises the practical issue of how to estimate τ. This issue is not addressed in this paper. The following theorem concludes this section.

THEOREM 6.3 (CPF with delay). *Consider system Σ that is obtained by putting together the n PF subsystems satisfying Assumption 2.2 and the coordination subsystems studied in Lemma 6.1 or 6.2. Then, the complete system Σ is ISS with input u_1. In particular, PF errors $\|e_i\|$ tend to some ball around zero, and the coordination errors $|\gamma_i - \gamma_j|$ and the speed tracking errors $|\gamma_i - v_L^*|$ converge to zero exponentially.*

Proof. Using Lemma 6.1 or 6.2, we conclude that $\tilde{v}_{r_i} = v_{r_i} - v_L = \dot{\gamma}_i - v_L$ converges to $v_L - v_L^*$ exponentially. Close examination of (2.7) shows that the PF and coordination control subsystems form an interconnected cascade system where $\tilde{v}_{r_i}$ is the output of the coordination control (CC) subsystem and the input to the PF subsystems. Since that latter is ISS from input $\tilde{v}_{r_i}$, the results follow. $\square$

The exposition in this section was strongly motivated by previous work on agreement problems for systems with delays. Especially relevant are the results available in [40] and [8], [10] for continuous time and discrete time, respectively. In particular, the results in [40] address the unforced version of (6.2), that is, with $\mathbf{v}_L(\gamma, t) = \mathbf{0}$. The results in this section reformulate those in [40] to the case where the agreement dynamics are forced by $\mathbf{v}_L(\gamma, t)$.

7. Illustrative example. This section presents an example that illustrates the application of the CPF techniques developed for the control of three AUVs.

7.1. CPF of three underactuated AUVs. Consider the problem of CPF control of three underactuated AUVs. Vehicle 2 is allowed to communicate with vehicles 1 and 3, but the latter two do not directly communicate between themselves. To simulate losses in the communications, we considered the situation where both

links fail 75% of the time, with the failures occurring periodically with a period of 10[sec]. Moreover, the information transmission delay is 5[sec]. Notice that during failures all the links become deactivated. Since in this scenario the valencies of the nodes vanish periodically, we apply the results of Lemma 6.2. In the simulations, we used the control law (6.9) with $k = 0.1[\text{sec}^{-1}]$.

7.1.1. AUV model. Consider an underactuated vehicle modeled as a rigid body subject to external forces and torques. (See [19] for details on vehicle modeling.) Let {I} be an inertial coordinate frame and {B} a body-fixed coordinate frame whose origin is located at the center of mass of the vehicle. The configuration $(R, \mathbf{p})$ of the vehicle is an element of the special Euclidean group $SE(3) := SO(3) \times \mathbb{R}^3$, where $R \in SO(3) := \{R \in \mathbb{R}^{3 \times 3} : RR^T = I_3, \det(R) = +1\}$ is a rotation matrix that describes the orientation of the vehicle and maps body coordinates into inertial coordinates, and $\mathbf{p} \in \mathbb{R}^3$ is the position of the origin of {B} in {I}. Denote by $\nu \in \mathbb{R}^3$ and $\omega \in \mathbb{R}^3$ the linear and angular velocities of the vehicle relative to {I} expressed in {B}, respectively. The following kinematic relations apply:

$$(7.1a) \qquad\qquad\qquad \dot{\mathbf{p}} = R\nu,$$

$$(7.1b) \qquad\qquad\qquad \dot{R} = RS(\omega),$$

where

$$S(x) := \begin{bmatrix} 0 & -x_3 & x_2 \\ x_3 & 0 & -x_1 \\ -x_2 & x_1 & 0 \end{bmatrix} \quad \forall x := (x_1, x_2, x_3)^T \in \mathbb{R}^3.$$

We consider underactuated vehicles with dynamic equations of motion of the form

$$(7.2a) \qquad\qquad \mathbf{M}\dot{\nu} = -S(\omega)\mathbf{M}\nu + f_\nu(\nu, \mathbf{p}, R) + B_1 u_1,$$

$$(7.2b) \qquad\qquad \mathbf{J}\dot{\omega} = f_\omega(\nu, \omega, \mathbf{p}, R) + B_2 u_2,$$

where $\mathbf{M} \in \mathbb{R}^{3 \times 3}$ and $\mathbf{J} \in \mathbb{R}^{3 \times 3}$ denote constant symmetric positive definite mass and inertia matrices, respectively. $u_1 \in \mathbb{R}$ and $u_2 \in \mathbb{R}^3$ denote the control inputs, which act upon the system through a constant nonzero vector $B_1 \in \mathbb{R}^3$ and a constant non-singular matrix $B_2 \in \mathbb{R}^{3 \times 3}$, respectively; and $f_\nu(\cdot)$, $f_\omega(\cdot)$ represent all the remaining forces and torques acting on the body. For the special case of an underwater vehicle, $\mathbf{M}$ and $\mathbf{J}$ also include the so-called hydrodynamic added-mass M_A and added-inertia J_A matrices, respectively, i.e., $\mathbf{M} = M_{RB} + M_A$, $\mathbf{J} = J_{RB} + J_A$, where M_{RB} and J_{RB} are the rigid-body mass and inertia matrices, respectively.

A solution to the PF problem (defined in section 2) of an AUV was given in [1], [2], where the control laws require that $\dot{\gamma}_i$ and $\ddot{\gamma}_i$ be known. Recall that we decomposed the desired speed profile into two parts as $v_{r_i} = v_L + \tilde{v}_{r_i}$ in which only the derivatives of v_L can be computed accurately. However, it can be shown that in the control laws of [1], [2], if the terms $\dot{\gamma}_i$ and $\ddot{\gamma}_i$ are replaced with v_L and $\dot{v}_L$, respectively, the resulting PF closed-loop system becomes ISpS from $\tilde{v}_{r_i}$ as an input. This leads to the following result.

THEOREM 7.1 (PF-AUV). *Consider an underactuated AUV with the equations of motion given by (7.1) and (7.2) and a desired path $\mathbf{p}_d(\gamma)$ in 3D-space to be followed. There is a control law for u_1 and u_2 as functions of the local states $\mathbf{p}_d$ and v_L that makes the closed-loop system satisfy Assumption 2.2.*
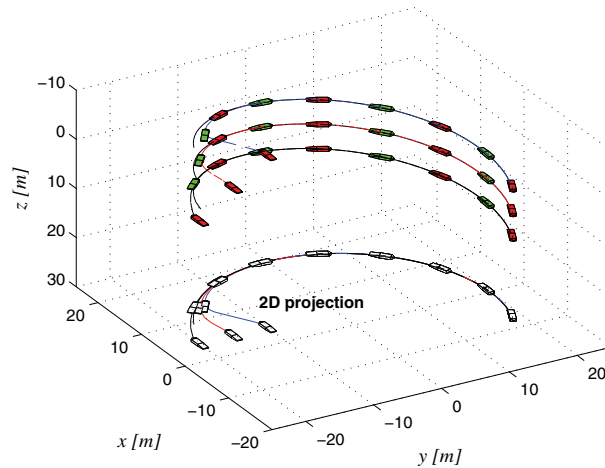
Proof. See the appendix. ☐

FIG. 4. *CPF of three AUVs, with communication losses and delay.*

Remark 7.2. It is important to notice that the particular PF algorithm that we derive yields input-to-state practical stability, not input-to-state stability. However, the key results obtained in the paper hold true, for input-to-state practical stability can always be viewed as an input-to-state stability condition with an extra constant input.

7.1.2. Simulations. In the simulations, the AUVs are required to follow three similar spatial paths shifted along the depth coordinate; that is, the paths are of the form

$$\mathbf{p}_{d_i}(\gamma_i) = \left[c_1 \cos\left(\frac{2\pi}{T}\gamma_i + \phi_d\right), c_1 \sin\left(\frac{2\pi}{T}\gamma_i + \phi_d\right), c_2\gamma_i + z_{0_i} \right],$$

with $c_1 = 20\,\text{m}$, $c_2 = 0.05\,\text{m}$, $T = 400$, $\phi_d = -\frac{3\pi}{4}$ and $z_{0_1} = -10\,\text{m}$, $z_{0_2} = -5\,\text{m}$, $z_{0_3} = 0\,\text{m}$. The initial conditions are $\mathbf{p}_1 = (5\,\text{m}, -10\,\text{m}, -5\,\text{m})$, $\mathbf{p}_2 = (5\,\text{m}, -15\,\text{m}, 0\,\text{m})$, $\mathbf{p}_3 = (5\,\text{m}, -20\,\text{m}, 5\,\text{m})$, $R_1 = R_2 = R_3 = I$, and $v_1 = v_2 = v_3 = \omega_1 = \omega_2 = \omega_3 = \mathbf{0}$. The reference speed v_L was set to $v_L = 0.5[\text{sec}^{-1}]$.

The vehicles are also required to keep a formation pattern that consists of having them aligned along a common vertical line. Figure 4 shows the trajectories of the AUVs. Figure 5 illustrates the evolution of the coordination and PF errors when the communication links fail periodically. Clearly, the vehicles adjust their speeds to meet the formation requirements, and the coordination errors $\gamma_{12} := \gamma_1 - \gamma_2$ and $\gamma_{13} := \gamma_1 - \gamma_3$ converge to zero.

8. Conclusions. This paper addressed the problem of steering a group of vehicles along given paths while holding a desired intervehicle formation pattern (coordinated path-following), all in the presence of *communication losses and time delays*. The solution proposed builds on Lyapunov-based techniques and addresses explicitly the constraints imposed by the topology of the intervehicle communications network. The problem of temporary communication failures was addressed under two scenarios: "brief connectivity losses" and "connected in mean" communication graphs. With the framework adopted, path-following and coordinated control system design become

(a) Path-following errors
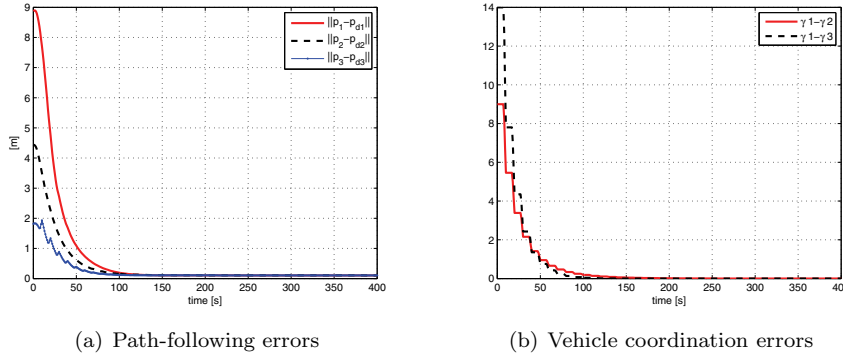

(b) Vehicle coordination errors

FIG. 5. *75% of temporal communication losses; time delay 5[sec].*

partially decoupled. As a consequence, the dynamics of each autonomous underwater vehicle can be dealt with by each vehicle controller locally, at the path-following control level. Coordination can then be achieved by resorting to a decentralized control law whereby the exchange of data among the vehicles is kept at a minimum. The system obtained by putting together the path-following and the vehicle coordination strategies proposed was shown to be either a feedback interconnection or a cascade of two input-to-state stable systems. Stability and convergence properties of the resulting interconnected system were studied formally by introducing a new small-gain theorem for systems with brief instabilities. Simulations illustrated the efficacy of the solution proposed.

Further work is required to extend the methodology proposed to tackle more complex coordination control problems, namely, coordinated control in the presence of stringent communication constraints that arise in the underwater world such as nonhomogeneous time variable delays, tight energy budgets, and reduced channel capacity. In particular, the study of coordinated path-following control systems yielding quantifiable measures of performance in the case of unidirectional, event driven communications, is warranted.

Appendix.

Proof of Lemma 3.2.

1. Since $\mathrm{Rank}(I - \mathcal{L}_\beta) = 1$, $\mathcal{L}_\beta$ has $n - 1$ eigenvalues at 1. Using the definition of $\mathcal{L}_\beta$, it can be easily verified that $\mathcal{L}_\beta \mathbf{1} = \mathbf{0}$ and $\beta^T \mathcal{L}_\beta = \mathbf{0}^T$, that is, zero is an eigenvalue. Therefore, we can conclude that zero is a single eigenvalue.

2. $\mathcal{L}_\beta K L_p = (K - \frac{1}{\beta^T \mathbf{1}} \mathbf{1}\mathbf{1}^T) L_p = K L_p$, since $\mathbf{1}^T L_p = \mathbf{0}^T$.

3. Straightforward computations show that $\mathcal{L}_\beta^T K^{-1} \mathcal{L}_\beta = K^{-1} - \frac{1}{\beta^T \mathbf{1}} \beta \beta^T$. Therefore, $\nu^T \mathcal{L}_\beta^T K^{-1} \mathcal{L}_\beta \nu = \nu^T K^{-1} \nu - \frac{1}{\beta^T \mathbf{1}} \nu^T \beta \beta^T \nu \leq \nu^T K^{-1} \nu$ for any $\nu \in \mathbb{R}^n$ and the equality holds for $\beta^T \nu = 0$, thus proving the result.

4. The result follows from the fact that $\tilde{\gamma} = \mathcal{L}_\beta \gamma$, $\mathcal{L}_\beta \mathbf{1} = \mathbf{0}$, and $\mathrm{Rank}\, \mathcal{L}_\beta = n - 1$.

5. This follows from the definition of $\tilde{\gamma}$ in (3.4).

6. This follows from the definition of $\tilde{\gamma}$ and the fact that $L_p \mathbf{1} = \mathbf{0}$.

7. From

$$|\tilde{\gamma}_i - \tilde{\gamma}_j|^2 = \tilde{\gamma}_i^2 + \tilde{\gamma}_j^2 - 2\tilde{\gamma}_i \tilde{\gamma}_j \leq 2(\tilde{\gamma}_i^2 + \tilde{\gamma}_j^2) \leq 2\|\tilde{\gamma}\|^2 < 2\epsilon^2$$

and $\tilde{\gamma}_i - \tilde{\gamma}_j = \gamma_i - \gamma_j$ it follows that $|\gamma_i - \gamma_j| < \sqrt{2}\epsilon$. Furthermore, from

$KL_p\gamma = KL_p\tilde{\gamma}$ it follows that $\|KL_p\gamma\| \le \|K\|.\|L_p\|.\|\tilde{\gamma}\| \le n\epsilon\|K\|$, where we used the fact that $\|L_p\| \le n$ and equality occurs for a complete graph, that is, for $p = [1, \dots, 1]^T$.

8. Recall the fact that if a graph is connected ($p \in P_c$), then L_p has a single eigenvalue at zero associated to the (right and left) eigenvector $\mathbf{1}$, and the rest of the eigenvalues are positive. Let L be a representative graph Laplacian of L_p for $p \in P_c$. Then, there is a unitary matrix $U = [u_1, \dots, u_n]$ with $u_1 = \frac{1}{\sqrt{n}}\mathbf{1}$ and a diagonal matrix $\Lambda = \mathrm{diag}[\lambda_1, \lambda_2, \dots, \lambda_n]$ with $0 = \lambda_1 < \lambda_2 \le \cdots \le \lambda_n$ such that $L = U\Lambda U^T$. For any $\nu \in \mathbb{R}^n$,

$$\nu^T L \nu = \sum_{i=1}^{n} \lambda_i (u_i^T \nu)^2$$

$$= \sum_{i=2}^{n} \lambda_i (u_i^T \nu)^2$$

$$\ge \lambda_2 \sum_{i=2}^{n} (u_i^T \nu)^2$$

$$= \lambda_2 \sum_{i=1}^{n} (u_i^T \nu)^2 - \lambda_2 (u_1^T \nu)^2$$

$$= \lambda_2 \nu^T \nu - \lambda_2 \frac{1}{n}(\mathbf{1}^T \nu)^2.$$

To compute $\lambda_{2,m}$, simply observe that the second term on the right-hand side of the inequality above is zero. Therefore, $\lambda_{2,m}$ is the minimum λ_2 over $p \in P_c$. If $\beta \ne \mathbf{1}$, a standard minimization of the vector function $\nu^T \nu - \frac{1}{n}(\mathbf{1}^T \nu)^2$ with constraints $\beta^T \nu = 0$ and $\nu^T \nu = 1$ yields the results. Similarly, it can be shown that $\bar{\lambda}_m > 0$. Simple numerical computations show that $\lambda_{2,m} = \bar{\lambda}_m$.

9. Recall that the graph Laplacian is $L = D - A$. Using the definitions of degree matrix D and adjacency matrix A, the result follows easily.

10. Because $v_L(\gamma_i, t)$ is bounded and Lipschitz, $|v_L(\gamma_i, t) - v_L(\gamma_j, t)| \le 2v_M$ and $|v_L(\gamma_i, t) - v_L(\gamma_j, t)| \le l|\gamma_i - \gamma_j| = l|\tilde{\gamma}_i - \tilde{\gamma}_j| \le \sqrt{2}l\|\tilde{\gamma}\|$. Then, using

$$\|\mathcal{L}_\beta \mathbf{v}_L(\gamma, t)\|^2 = \sum_{i=1}^{n} \left(\sum_{j=1}^{n} \frac{v_L(\gamma_i, t) - v_L(\gamma_j, t)}{\sigma_j} \right)^2,$$

where $\sigma_j = k_j \sum_i \frac{1}{k_i}$, it is easy to show that $\|\mathcal{L}_\beta \mathbf{v}_L(\gamma, t)\| \le \sqrt{2n}l\|\tilde{\gamma}\|$ and $\|\mathcal{L}_\beta \mathbf{v}_L(\gamma, t)\| \le 2\sqrt{n}v_M$, and the result follows.

Proof of Lemma 5.1. First we show that

$$\text{(A.1)} \qquad \sum_{i=1}^{n} |\tilde{v}_{r_i}|^2 = \tilde{\gamma}^T L_p K^2 L_p \tilde{\gamma} \le n^2 k_M^2 \|\tilde{\gamma}\|^2,$$

where $\tilde{v}_{r_i}$ and $\tilde{\gamma}$ are as defined in (5.2) and (3.4), respectively. Denote by $l_{i,p}$ the ith column (or row) of L_p. Then $\tilde{v}_{r_i} = k_i l_{i,p}^T \gamma$ and

$$\sum_i |\tilde{v}_{r_i}|^2 = \sum_i k_i^2 \gamma^T l_{i,p} l_{i,p}^T \gamma$$

$$= \gamma^T \sum_i k_i^2 l_{i,p} l_{i,p}^T \gamma$$

$$= \gamma^T L_p K^2 L_p \gamma$$

$$= \tilde{\gamma}^T L_p K^2 L_p \tilde{\gamma}.$$

Now, consider n PF subsystems, each satisfying Assumption 2.2, and let $\zeta = [\zeta_i]_{n \times 1}$ and $V_1 = \sum_i W_i$. Using (2.6), (2.7), and (A.1) yields

$$\underline{\alpha}_1 \|\zeta\|^2 \le V_1 \le \bar{\alpha}_1 \|\zeta\|^2,$$
$$\dot{V}_1 \le -\lambda_1 V_1 + \rho_1 n^2 k_M^2 \|\tilde{\gamma}\|^2 + u_1^2.$$

Integrating the above differential inequality, the ISS property (5.6) follows.

Proof of Proposition 4.1 (*system interconnection*). Define $V = V_1 + aV_2$ for some $a > 0$ to be chosen later. Clearly, V satisfies the first condition of (4.6) for some $\underline{\alpha} > 0$, $\bar{\alpha} > 0$. Next, we will show that the second condition is also satisfied. Taking the derivative of V yields

$$\dot{V} \le -\left(\lambda_1 - \frac{a\rho_2}{\underline{\alpha}_1}\right) V_1 - a\left(\lambda_2 - \frac{\rho_1}{a\underline{\alpha}_2}\right) V_2 + g\|d\|^2,$$

where $g = \max(1, a)$. At this stage assume ρ_1 and ρ_2 are nonzero, and let

$$(A.2) \qquad \lambda_0 = \lambda_1 - \frac{a\rho_2}{\underline{\alpha}_1} = \lambda_2 - \frac{\rho_1}{a\underline{\alpha}_2}.$$

Consider the case where $\lambda_2(t) = \lambda_2 > 0$ is constant. If $\rho_1\rho_2 < \underline{\alpha}_1\underline{\alpha}_2\lambda_1\lambda_2$, there exist positive numbers λ_0 and a satisfying (A.2). As a consequence, $\dot{V} \le -\lambda_0 V + g\|d\|^2$, the interconnected system is ISS with input d, and the convergence rate is $\lambda = \lambda_0$.

Consider now the case where $\lambda_2(t)$ is not constant and system 2 has brief instabilities characterized by $\chi(p)$ and $\lambda_2(t)$ as in (4.3). Using the same Lyapunov function $V = V_1 + aV_2$ and λ_0 as in (A.2), compute the derivative of V to obtain

$$\dot{V} \le -\lambda_0 V + a(\lambda_2 - \lambda_2(t))V_2 + g\|d\|^2$$

that yields

$$\dot{V} \le \begin{cases} -\lambda_0 V + g\|d\|^2, & \chi(p) = 0, \\ (\lambda_3 - \lambda_0)V + g\|d\|^2, & \chi(p) = 1, \end{cases}$$

where $\lambda_3 := \lambda_2 + \tilde{\lambda}_2$. Again, λ_0 exists if $\rho_1\rho_2 < \underline{\alpha}_1\underline{\alpha}_2\lambda_1\lambda_2$. Rewrite

$$\dot{V} \le -\lambda_0 V + a(\lambda_2 - \lambda_2(t))V_2 + g\|d\|$$

and use $aV_2 = V - V_1$ to derive

$$\dot{V} \le -(\lambda_0 - \lambda_3\chi(p))V + g\|d\|^2,$$

where $\lambda_3 := \lambda_2 + \tilde{\lambda}_2$. Integrating the above differential inequalities, it is easy to show that

$$V(t) \le V(t_0)e^{-\lambda_0(t-t_0)+\lambda_3 T_p} + g\sup_{[t_0,t]} \|d\|^2 \int_{t_0}^t e^{-\lambda_0(t-\tau)+\lambda_3 T_p} d\tau.$$

This yields

$$V(t) \le V(t_0)e^{-(\lambda_0-\alpha\lambda_3)(t-t_0)+\lambda_3 T_\alpha} + \frac{e^{\lambda_3 T_\alpha}}{\lambda_0 - \alpha\lambda_3} g\sup_{[t_0,t]} d^2,$$

where $T_\alpha = (1-\alpha)T_0$ if the system has brief instabilities as defined in (3.3). Therefore, the interconnected system is ISS with d as input if $\alpha < \lambda_0/\lambda_3$.

Suppose now that $\rho_2 = 0$ and $\rho_1 > 0$. In this case, the interconnected system takes a cascade configuration and the dynamics of system 2 are reduced to

$$\dot{V}_2 \leq \begin{cases} -\lambda_2 V_2 + d_2^2, & \chi(p) = 0, \\ \tilde{\lambda}_2 V_2 + d_2^2, & \chi(p) = 1, \end{cases}$$

whose solution takes the form

$$V_2(t) \leq V_2(t_0)e^{-(\lambda_2-\alpha\lambda_3)(t-t_0)+\lambda_3 T_\alpha} + \frac{e^{\lambda_3 T_\alpha}}{\lambda_2 - \alpha\lambda_3}\sup_{[t_0,t]} d_2^2.$$

Using the above inequality together with (4.1) and (4.2) it is easy to obtain

$$V_1(t) \leq a_1 e^{-\lambda_1 t} + a_2 e^{-(\lambda_2-\alpha\lambda_3)t} + a_3 \sup_{[t_0,t]}\|d\|^2$$

for some $a_i \geq 0$, $i = 1, 2, 3$. Therefore, the cascade system is ISS with d as input if $\alpha < \lambda_2/\lambda_3$ and the convergence rate will be $\min(\lambda_1, \lambda_2 - \alpha\lambda_3)$.

Proof of (5.15). The objective is to make $\bar{\lambda}_0 > 0$, that is, $\lambda_\alpha - c_1 l\sqrt{2n} > 0$. Replacing $c_1 = \sqrt{ck_M/k_m}$ in the above inequality yields

$$\lambda_\alpha - l\sqrt{2n}e^{\lambda_\alpha \bar{T}_0}\sqrt{\frac{k_M}{k_m}} > 0.$$

The left-hand side of the inequality takes its maximum at

$$\lambda_\alpha = \frac{1}{\bar{T}_0}\ln\left(\frac{1}{l\sqrt{2n}\bar{T}_0}\sqrt{\frac{k_m}{k_M}}\right),$$

from which it follows that

$$\max \bar{\lambda}_0 = \frac{1}{\bar{T}_0}\ln\left(\frac{1}{el\sqrt{2n}\bar{T}_0}\sqrt{\frac{k_m}{k_M}}\right).$$

To make $\bar{\lambda}_0$ positive it is required that

$$\frac{1}{el\bar{T}_0}\sqrt{\frac{k_m}{2nk_M}} > 1.$$

Using $\bar{T}_0 \leq T + \tau_D$ gives

$$l\sqrt{\frac{k_M}{k_m}} < \frac{1}{e(T+\tau_D)\sqrt{2n}},$$

from which the result follows.

Proof of Theorem 7.1. *PF of an underactuated AUV.* The methodology adopted for PF control system design is rooted in Lyapunov-based and backstepping techniques. The exposition that follows is based on the work in [2].

Step 1. Define the global diffeomorphic coordinate transformation

$$\mathbf{e} := R^T[\mathbf{p} - \mathbf{p}_d(\gamma_i)],$$

which expresses the path tracking error $\mathbf{p} - \mathbf{p}_d$ in a body-fixed frame. For simplicity of presentation, we will for the most part drop the index i in this section. Recall the definition of speed tracking error $\eta = \dot{\gamma}_i - v_r$, where v_r is a reference speed profile. Recall also how the reference speed v_r is decomposed as $v_r = v_L + \tilde{v}_r$, where the derivatives of v_L are known but those of $\tilde{v}_r$ are not. The derivative of $\mathbf{e}$ yields

$$\dot{\mathbf{e}} = -S(\omega)\mathbf{e} + \nu - v_L R^T \mathbf{p}_d^\gamma - \tilde{\eta} R^T \mathbf{p}_d^\gamma,$$

where $\tilde{\eta} := \eta + \tilde{v}_r$ (or equivalently $\dot{\gamma}_i = v_L + \tilde{\eta}$) and superscript γ stands for partial derivative with respect to γ. For example, $\mathbf{p}_d^\gamma = \frac{\partial \mathbf{p}_d}{\partial \gamma}$ and $\mathbf{p}_d^{\gamma^2} = \frac{\partial^2 \mathbf{p}_d}{\partial \gamma^2}$.

We define the Lyapunov function $W_1 := \frac{1}{2}\mathbf{e}^T \mathbf{e}$ and compute its time derivative to obtain

$$\dot{W}_1 = \mathbf{e}^T(\nu - v_L R^T \mathbf{p}_d^\gamma) - \tilde{\eta}\mathbf{e}^T R^T \mathbf{p}_d^\gamma,$$

where we used the fact that $\mathbf{e}^T S(\omega)\mathbf{e} = 0 \ \forall \mathbf{e}, \omega \in \mathbb{R}^3$. We regard ν as a virtual control signal and introduce the virtual control tracking error variable

$$z_1 := \nu - v_L R^T \mathbf{p}_d^\gamma + k_e M^{-1} \mathbf{e}.$$

Then, $\dot{W}_1$ can be rewritten as

$$\dot{W}_1 = -k_e \mathbf{e}^T M^{-1} \mathbf{e} + \mathbf{e}^T z_1 + \alpha_1 \tilde{\eta},$$

where $\alpha_1 := -\mathbf{e}^T R^T \mathbf{p}_d^\gamma$. Ideally, in the absence of $\tilde{\eta}$ one would like to drive z_1 to zero so as to render $\dot{W}_1$ negative. This motivates the next step.

Step 2. The time derivative of z_1 yields

$$M\dot{z}_1 = v_L \Gamma \omega + S(M z_1)\omega + B_1 u_1 + \tilde{\eta} h_1 + h_2,$$

where

$$\begin{aligned}
\Gamma &:= MS(R^T \mathbf{p}_d^\gamma) - S(M R^T \mathbf{p}_d^\gamma), \\
h_1 &:= -v_L M R^T \mathbf{p}_d^{\gamma^2} - v_L^\gamma M R^T \mathbf{p}_d^\gamma - k_e R^T \mathbf{p}_d^\gamma, \\
h_2 &:= f_\nu + k_e \nu + v_L h_1.
\end{aligned}$$

It turns out that due to lack of actuation, it is not always possible to drive z_1 to zero. Instead, we drive z_1 to a constant design vector $\delta \in \mathbb{R}^3$. To this effect, we define a new error vector $\phi := z_1 - \delta$ and the augmented Lyapunov function

$$W_2 := W_1 + \frac{1}{2}\phi^T M^2,$$

whose derivative is

$$\dot{W}_2 = -k_e \mathbf{e}^T M^{-1} \mathbf{e} + \mathbf{e}^T \delta + \phi^T M(B\zeta + M^{-1}\mathbf{e} + h_2) + \alpha_2 \tilde{\eta},$$

with $\alpha_2 := \alpha_1 + \phi^T M h_1$,

$$B := \begin{pmatrix} B_1 & S(M\delta) + v_L \Gamma \end{pmatrix}, \text{ and } \zeta := \begin{pmatrix} u_1 \\ \omega \end{pmatrix},$$

where we used the fact that $\phi^T M S(M z_1)\omega = \phi^T M S(M\delta)\omega$. Matrix B can always be made full rank; see [2] for details. Let

$$\beta_1 := B^T (BB^T)^{-1}(-h_2 - M^{-1}\mathbf{e} - k_\phi \phi).$$

To complete this step, we set u_1 to be the first entry of β_1, that is, $u_1 = \begin{pmatrix} 1 & 0_{1\times 3} \end{pmatrix}\beta_1$, and introduce the error variable

$$z_2 := \omega - \Pi\beta_1, \quad \Pi := \begin{pmatrix} 0_{3\times 1} & I_{3\times 3} \end{pmatrix}$$

that should be driven to zero. It follows that

$$\dot{W}_2 = -k_e \mathbf{e}^T M^{-1}\mathbf{e} + \mathbf{e}^T \delta - k_\phi \phi^T M\phi + \phi^T MB\Pi^T z_2 + \alpha_2\tilde{\eta}.$$

Step 3. Let $\dot{\beta}_1 := h_3 + h_4\tilde{\eta}$, where h_3 collects the terms in $\dot{\beta}_1$ not containing $\tilde{\eta}$. For simplicity we do not expand h_3 and h_4. Define

$$W_3 := W_2 + \frac{1}{2}z_2^T J z_2,$$

whose time derivative, after applying the control law

$$u_2 = B_2^{-1}(-f_\omega + J\Pi h_3 - \Pi B^T M\phi - k_z z_2),$$

yields

(A.3) $$\dot{W}_3 = -k_e \mathbf{e}^T M^{-1}\mathbf{e} + \mathbf{e}^T \delta - k_\phi \phi^T M\phi - k_z z_2^T z_2 + \alpha_3\tilde{\eta},$$

where $\alpha_3 = \alpha_2 - z_2^T J\Pi h_4$. At this point it is important to notice that

(A.4) $$|\alpha_3| \leq k_1\|\mathbf{e}\| + k_2\|\phi\| + k_3\|z_2\|$$

for some $k_i > 0$, $i = 1, 2, 3$, that are functions of v_L, v_L^γ, M, $\mathbf{p}_d^\gamma$, and $\mathbf{p}_d^{\gamma^2}$. The design phase is concluded at this step for the case where $\eta = 0$ simply by making $\dot{\gamma}_i = v_r$. In this case, $\tilde{\eta} = \tilde{v}_r$ and

$$\dot{W}_3 \leq -\lambda W_3 + \rho_1\|\delta\|^2 + \rho_2|\tilde{v}_r|$$

for some $\lambda > 0$, $\rho_1 > 0$, and $\rho_2 > 0$. That is, the PF closed-loop system is ISpS with input $\tilde{v}_r$, state $x_1 = (\mathbf{e}, \phi, z_2)^T$, and constant $\rho_1\|\delta\|^2$.

Step 4. This extra step contemplates the situation where $\eta \neq 0$. To this effect, augment the Lyapunov function W_3 to obtain

$$W_4 := W_3 + \frac{1}{2}\eta^2 = \frac{1}{2}\mathbf{e}^T\mathbf{e} + \frac{1}{2}\phi^T M^2\phi + \frac{1}{2}z_2^T J z_2 + \frac{1}{2}\eta^2.$$

Set the feedback law

$$\dot{\eta} = -\alpha_3 - k_\eta\eta$$

to make

$$\dot{W}_4 = -k_e \mathbf{e}^T M^{-1}\mathbf{e} - k_\phi \phi^T M\phi - k_z z_2^T z_2 - k_\eta\eta^2 + \mathbf{e}^T\delta + \alpha_3\tilde{v}_r,$$

which can be rewritten as

(A.5) $$\dot{W}_4 \leq -\lambda W_4 + \rho_1\|\delta\|^2 + \rho_2|\tilde{v}_r|$$

for some $\lambda > 0$, $\rho_1 > 0$, and $\rho_2 > 0$. Again, this makes the closed-loop system ISpS with input $\tilde{v}_r$, state $x_1 = (\mathbf{e}, \phi, z_2, \eta)^T$, and constant $\rho_1\|\delta\|^2$.

REFERENCES

[1] A. P. Aguiar and J. P. Hespanha, *Logic-based switching control for trajectory-tracking and path-following of underactuated autonomous vehicles with parametric modeling uncertainty*, in Proceedings of the American Control Conference, Boston, MA, 2004, pp. 3004–3010.

[2] A. P. Aguiar and J. P. Hespanha, *Trajectory-tracking and path-following of underactuated autonomous vehicles with parametric modeling uncertainty*, IEEE Trans. Automat. Control, 52 (2007), pp. 1362–1379.

[3] A. P. Aguiar, J. P. Hespanha, and P. Kokotovic, *Path-following for non-minimum phase systems removes performance limitations*, IEEE Trans. Automat. Control, 50 (2005), pp. 234–239.

[4] A. P. Aguiar, I. Kaminer, R. Ghabcheloo, A. M. Pascoal, N. Hovakimyan, C. Cao, and V. Dobrokhodov, *Coordinated path following of multiple UAVs for time-critical missions in the presence of time-varying communication topologies*, in Proceedings of the 17th IFAC World Congress, Korea, 2008, pp. 16015–16020.

[5] M. Arkak, *Passivity as a design tool for group coordination*, IEEE Trans. Automat. Control, 52 (2007), pp. 1380–1390.

[6] R. Beard, J. Lawton, and F. Hadaegh, *A coordination architecture for spacecraft formation control*, IEEE Trans. Control Systems Tech., 9 (2001), pp. 777–790.

[7] D. P. Bertsekas and J. N. Tsitsiklis, *Parallel and Distributed Computation: Numerical Methods*, Prentice–Hall, Englewood Cliffs, NJ, 1989.

[8] V. D. Blondel, J. M. Hendrickx, A. Olshevsky, and J. N. Tsitsiklis, *Convergence in multiagent coordination, consensus, and flocking*, in Proceedings of the 44th IEEE CDC-ECC, Seville, Spain, 2005, pp. 2996–3000.

[9] M. Cao, A. S. Morse, and B. D. O. Anderson, *Agreeing asynchronously: Announcement of results*, in Proceedings of the 46th IEEE Conference on Decision and Control, San Diego, CA, 2006, pp. 4301–4306.

[10] M. Cao, A. S. Morse, and B. D. O. Anderson, *Reaching an agreement using delayed information*, in Proceedings of the 46th IEEE Conference on Decision and Control, San Diego, CA, 2006, pp. 3375–3380.

[11] M. Cao, A. S. Morse, and B. D. O. Anderson, *Reaching a consensus in a dynamically changing environment: Convergence rates, measurement delays, and asynchronous events*, SIAM J. Control Optim., 47 (2008), pp. 601–623.

[12] J. Cortes and F. Bullo, *Coordination and geometric optimization via distributed dynamical systems*, SIAM J. Control Optim., 44 (2005), pp. 1543–1574.

[13] T. B. Curtin, J. G. Bellingham, J. Catipovic, and D. Webb, *Autonomous oceanographic sampling network*, Oceanography, 6 (1993), pp. 86–95.

[14] D. V. Dimarogonas, S. G. Loizou, K. J. Kyriakopoulos, and M. M. Zavlanos, *A feedback stabilization and collision avoidance scheme for multiple independent non-point agents*, Automatica, 42 (2006), pp. 229–243.

[15] W. B. Dunbar and R. M. Murray, *Distributed receding horizon control for multi-vehicle formation stabilization*, Automatica, 42 (2006), pp. 549–558.

[16] M. Egerstedt and X. Hu, *Formation constrained multi-agent control*, IEEE Trans. Robotics and Automation, 17 (2001), pp. 947–951.

[17] P. Encarnação and A. Pascoal, *Combined trajectory tracking and path following: An application to the coordinated control of marine craft*, in Proceedings of the 40th IEEE Conference on Decision and Control (CDC), Orlando, FL, 2001, pp. 964–969.

[18] A. Fax and R. Murray, *Information flow and cooperative control of vehicle formations*, IEEE Trans. Automat. Control, 49 (2004), pp. 1465–1476.

[19] T. Fossen, *Guidance and Control of Ocean Vehicles*, John Wiley & Sons, New York, 1994.

[20] R. Ghabcheloo, A. Aguiar, A. Pascoal, and C. Silvestre, *Synchronization in multi-agent systems with switching topologies and non-homogeneous communication delays*, in Proceedings of the 46th IEEE Conference on Decision and Control (CDC), New Orleans, LA, 2007, pp. 2327–2332.

[21] R. Ghabcheloo, A. Aguiar, A. Pascoal, C. Silvestre, I. Kaminer, and J. Hespanha, *Coordinated path-following control of multiple underactuated autonomous vehicles in the presence of communication failures*, in Proceedings of the 45th IEEE Conference on Decision and Control (CDC), San Diego, CA, 2006, pp. 4345–4350.

[22] R. Ghabcheloo, A. Pascoal, C. Silvestre, and I. Kaminer, *Nonlinear coordinated path-following control of multiple wheeled robots with bi-directional communication constraints*, Internat. J. Adapt. Control Signal Process., 21 (2007), pp. 133–157.

[23] F. Giuletti, L. Pollini, and M. Innocenti, *Autonomous formation flight*, IEEE Control Systems Mag., 20 (2000), pp. 33–34.

[24] C. Godsil and G. Royle, *Algebraic Graph Theory*, Grad. Texts in Math., Springer-Verlag, New York, 2001.

[25] J. M. Hespanha, O. A. Yakimenko, I. I. Kaminer, and A. M. Pascoal, *Linear parametrically varying systems with brief instabilities: An application to vision/inertial navigation*, IEEE Trans. Aerospace Electron. Systems, 40 (2004), pp. 889–900.

[26] I.-A. F. Ihle, *Coordinated Control of Marine Craft*, Ph.D. thesis, Norwegian University of Science and Technology, Trondheim, Norway, 2006.

[27] H. Ito, *A constructive proof of ISS small-gain theorem using generalized scaling*, in Proceedings of the 41st IEEE Conference on Decision and Control, Las Vegas, NV, 2002, pp. 2286–2291.

[28] A. Jadbabaie, J. Lin, and A. S. Morse, *Coordination of groups of mobile autonomous agents using nearest neighbor rules*, IEEE Trans. Automat. Control, 48 (2003), pp. 988–1001.

[29] I. Kaminer, O. Yakimenko, V. Dohrokhodov, A. Pascoal, N. Hovakimyan, V. Patel, C. Cao, and A. Young, *Coordinated path following for time-critical missions of multiple UAVs via L1 adaptive output feedback controllers*, in Proceedings of the AIAA Guidance, Navigation and Control Conference and Exhibit, Hilton Head, SC, Aug. 20–23, 2007, paper AIAA-2007-6409.

[30] I. Kaminer, O. Yakimenko, A. Pascoal, and R. Ghabcheloo, *Path generation, path following and coordinated control for time-critical missions of multiple UAVs*, in Proceedings of the American Control Conference (ACC), Minneapolis, MN, 2006, pp. 4906–4913.

[31] H. K. Khalil, *Nonlinear Systems*, 3rd ed., Prentice–Hall, Englewood Cliffs, NJ, 2002.

[32] Y. Kim and M. Mesbahi, *On maximizing the second smallest eigenvalue of state-dependent graph Laplacian*, IEEE Trans. Automat. Control, 51 (2006), pp. 116–120.

[33] D. J. Klein, C. Matlack, and K. A. Morgansen, *Cooperative target tracking using oscillator models in three dimensions*, in Proceedings of the American Control Conference, New York, 2007, pp. 2569–2575.

[34] E. Kyrkjebo, *Motion Coordination of Mechanical Systems: Leader-Follower Synchronization of Euler-Lagrange Systems Using Output Feedback Control*, Ph.D. thesis, Norwegian University of Science and Technology, Trondheim, Norway, 2007.

[35] L. Lapierre, D. Soetanto, and A. Pascoal, *Coordinated motion control of marine robots*, in Proceedings of the 6th IFAC Conference on Manoeuvring and Control of Marine Craft (MCMC), Girona, Spain, 2003.

[36] J. R. T. Lawton, R. W. Beard, and B. J. Young, *A decentralized approach to formation maneuvers*, IEEE Trans. Robotics and Automation, 19 (2003), pp. 933–942.

[37] Z. Lin, *Coupled Dynamic Systems: From Structure Towards Stability and Stabilizability*, Ph.D. thesis, University of Toronto, Toronto, ON, Canada, 2006.

[38] Z. Lin, B. Francis, and M. Maggiore, *State agreement for continuous-time coupled nonlinear systems*, SIAM J. Control Optim., 46 (2007), pp. 288–307.

[39] M. Mesbahi and F. Hadaegh, *Formation flying control of multiple spacecraft via graphs, matrix inequalities and switching*, J. Guidance Control Dynam., 24 (2001), pp. 369–377.

[40] L. Moreau, *Stability of continuous-time distributed consensus algorithm*, in Proceedings of the 43rd IEEE Conference on Decision and Control, Atlantis, Paradise Island, Bahamas, 2004, pp. 3998–4003.

[41] N. Moshtagh and A. Jadbabaie, *Distributed geodesic control laws for flocking of nonholonomic agents*, IEEE Trans. Automat. Control, 52 (2007), pp. 681–686.

[42] R. M. Murray, *Recent research in cooperative control of multi-vehicle systems*, ASME J. Dynam. Systems Measurement Control, 129 (2007), pp. 571–583.

[43] S. Nair and N. E. Leonard, *Stable synchronization of mechanical system networks*, SIAM J. Control Optim., 47 (2008), pp. 661–683.

[44] R. Olfati-Saber, J. A. Fax, and R. M. Murray, *Consensus and cooperation in networked multi-agent systems*, Proc. IEEE, 95 (2007), pp. 215–233.

[45] A. Olshevsky and J. N. Tsitsiklis, *On the nonexistence of quadratic Lyapunov functions for consensus algorithms*, IEEE Trans. Automat. Control, 53 (2008), pp. 2642–2645.

[46] A. Papachristodoulou and A. Jadbabaie, *Synchronization in oscillator networks: Switching topologies and non-homogeneous delays*, in Proceedings of the 44th IEEE Conference on Decision and Control (CDC), Seville, Spain, 2005, pp. 5692–5697.

[47] A. Pascoal et al., *Robotic ocean vehicles for marine science applications: The European ASIMOV project*, in Proceedings of the OCEANS MTS/IEEE Conference, Providence, RI, 2000, pp. 409–415.

[48] Q. C. Pham and J. J. E. Slotine, *Stable concurrent synchronization in dynamic system networks*, Neural Networks, 20 (2007), pp. 62–77.

[49] M. Pratcher, J. D'Azzo, and A. Proud, *Tight formation control*, J. Guidance Control Dynam., 24 (2001), pp. 246–254.

[50] A. Rahmani, M. Mesbahi, and F. Y. Hadaegh, *On the optimal balanced-energy formation flying maneuvers*, AIAA J. Guidance Control Dynam., 29 (2006), pp. 1395–1403.

[51] W. Ren and R. W. Beard, *Distributed Consensus in Multi-Vehicle Cooperative Control*, Comm. Control Engrg. Ser., Springer-Verlag, New York, 2007.

[52] W. Ren and N. Sorensen, *Distributed coordination architecture for multi-robot formation control*, J. Robotics and Autonomous Systems, 56 (2008), pp. 324–333.

[53] W. J. Rugh, *Linear System Theory*, Prentice–Hall, Englewood Cliffs, NJ, 1993.

[54] R. Sepulchre, D. A. Paley, and N. E. Leonard, *Stabilization of planar collective motion with all-to-all communication*, IEEE Trans. Automat. Control, 52 (2007), pp. 811–824.

[55] D. D. Šiljak, *Decentralized Control of Complex Systems*, Academic Press, Boston, MA, 1991.

[56] D. D. Šiljak, *Dynamic graphs*, Nonlinear Anal. Hybrid Systems, 2 (2008), pp. 544–567.

[57] R. Skjetne, T. I. Fossen, and P. Kokotovic, *Robust output maneuvering for a class of nonlinear systems*, Automatica, 40 (2004), pp. 373–383.

[58] R. Skjetne, S. Moi, and T. Fossen, *Nonlinear formation control of marine craft*, in Proceedings of the 41st IEEE Conference on Decision and Control, Las Vegas, NV, 2002, pp. 1699–1704.

[59] E. D. Sontag and Y. Wang, *New characterizations of input-to-state stability*, IEEE Trans. Automat. Control, 41 (1996), pp. 1283–1294.

[60] D. Stilwell and B. Bishop, *Platoons of underwater vehicles*, IEEE Control Systems Mag., 20 (2000), pp. 45–52.

[61] J. N. Tsitsiklis and M. Athans, *Convergence and asymptotic agreement in distributed decision problems*, IEEE Trans. Automat. Control, 29 (1984), pp. 42–50.

[62] C. Yu, J. M. Hendrickx, B. Fidan, and B. D. O. Anderson, *Three and higher dimensional autonomous formations: Rigidity, persistence and structural persistence*, Automatica, 43 (2007), pp. 387–402.

[63] F. Zhang, D. M. Fratantoni, D. Paley, J. Lund, and N. E. Leonard, *Control of coordinated patterns for ocean sampling*, Internat. J. Control, 80 (2007), pp. 1186–1199.

[64] F. Zhang and P. S. Krishnaprasad, *Co-ordinated orbit transfer of satellite clusters*, Astrodynamics, Space Missions and Chaos (Annals of the New York Academy of Sciences), 1017 (2004), pp. 112–137.